Wave *and* Tidal Energy

Edited by
Deborah **Greaves** | Gregorio **Iglesias**

WILEY

Wave and Tidal Energy

Wave and Tidal Energy

Edited by

Deborah Greaves

Professor of Ocean Engineering, School of Engineering,
University of Plymouth, UK

and

Gregorio Iglesias

Professor of Coastal Engineering, School of Engineering,
University of Plymouth, UK

WILEY

This edition first published 2018

Registered Offices
John Wiley & Sons, Inc., 111 River Street, Hoboken, NJ 07030, USA
John Wiley & Sons Ltd, The Atrium, Southern Gate, Chichester, West Sussex, PO19 8SQ, UK

Editorial Office
The Atrium, Southern Gate, Chichester, West Sussex, PO19 8SQ, UK

For details of our global editorial offices, customer services, and more information about Wiley products visit us at www.wiley.com.

Wiley also publishes its books in a variety of electronic formats and by print-on-demand. Some content that appears in standard print versions of this book may not be available in other formats.

Library of Congress Cataloging-in-Publication Data

Names: Greaves, Deborah, editor. | Iglesias, Gregorio, 1969– editor.
Title: Wave and tidal energy / edited by Deborah Greaves (University of Plymouth), Gregorio Iglesias (University of Plymouth).
Description: Hoboken, NJ : Wiley, 2018. | Includes bibliographical references and index. |
Identifiers: LCCN 2017042798 (print) | LCCN 2017051143 (ebook) | ISBN 9781119014454 (pdf) | ISBN 9781119014478 (epub) | ISBN 9781119014447 (cloth)
Subjects: LCSH: Ocean wave power. | Tidal power. | Water-power. | Renewable energy sources.
Classification: LCC TC147 (ebook) | LCC TC147 .W37 2018 (print) | DDC 621.31/2134–dc23
LC record available at https://lccn.loc.gov/2017042798

Cover design by Wiley
Cover images: (Waves) © kateafter/Gettyimages;(Rays) barbol88/Gettyimages

Set in 10/12pt Warnock by SPi Global, Pondicherry, India

Printed in Great Britain by TJ International Ltd, Padstow, Corwall

10 9 8 7 6 5 4 3 2 1

Contents

List of Contributors

Javier Abanades Tercero
Offshore Renewable Energy Consultant, TYPSA, Spain
Associate Researcher, School of Engineering, University of Plymouth, UK

Francisco Acuña
Chief Executive Officer, InTrust Global Investments LLC, Washington, D.C. USA

Sharay Astariz
Associate Researcher, University of Santiago de Compostela, Spain

Bradley Buckham
Department of Mechanical Engineering, University of Victoria, BC, Canada

Chenyu
Researcher, Ocean University of China, Qingdao, China

Curran Crawford
Department of Mechanical Engineering, University of Victoria, BC, Canada

Erica Cruz
Senior Researcher, WavEC – Offshore Renewables, Lisboa,
Portugal

Boel Ekergard
Seabased Industry AB, Sweden

Deborah Greaves
Professor of Ocean Engineering, School of Engineering, University of Plymouth, UK

John Griffiths
Associate, EMEC Ltd, Chair of UK National Committee on Wave & Tidal Standards

Martyn Hann
Lecturer in Coastal Engineering, School of Engineering, University of Plymouth, UK

Andrew J. Hillis
Senior Lecturer in Mechanical Engineering, Centre for Power Transmission and Motion Control, University of Bath, UK

Brian Holmes
MaREI Centre, Environmental Research Institute,
University College Cork, Ringaskiddy, Ireland

Gregorio Iglesias
Professor of Coastal Engineering, School of Engineering, University of Plymouth, UK

Lars Johanning
Professor of Ocean Technology, University of Exeter, Penryn Campus, UK

Kwangsoo Lee
Principal Research Scientist,
Institute of Ocean Science & Technology,
Korea

Mats Leijon
Professor, Uppsala University, Sweden

Inês Machado
Senior Researcher, WavEC – Offshore
Renewables, Lisboa, Portugal

Vanesa Magar
Centro de Investigación Científica y
Educación Superior de Ensenada
(CICESE), México

Dorleta Marina
BIMEP,
Lemoiz, Spain

Allan Mason-Jones
School of Engineering, Cardiff University,
Wales, UK

Daphne M. O'Doherty
School of Engineering, Cardiff University,
Wales, UK

Tim O'Doherty
School of Engineering, Cardiff University,
Wales, UK

Anne Marie O'Hagan
Senior Research Fellow, MaREI Centre,
Environmental Research Institute,
University College Cork, Ringaskiddy,
Ireland

Carlos Perez-Collazo
PRIMaRE Research Fellow, School of
Engineering, University of Plymouth, UK

Andrew R. Plummer
Professor of Machine Systems,
Centre for Power Transmission and
Motion Control, University of Bath, UK

Hongda Shi
Professor, Ocean University of China,
Qingdao, China

Sungwon Shin
Research Professor, Kangwon National
University, Korea

Teresa Simas
Senior Researcher, WavEC – Offshore
Renewables, Lisboa, Portugal

Phillip R. Thies
Senior Lecturer Renewable Energy,
University of Exeter, Penryn Campus,
UK

Yago Torre-Enciso
BIMEP, Lemoiz, Spain

Angela Vazquez
Associate Researcher, University of
Santiago de Compostela, Spain

Paul Vigars
Director of Teobi Engineering
Associates Ltd, UK (formerly Research
& Technology Manager at Alstom Ocean
Energy, UK)

Thomas Vyzikas
Associate Researcher,
School of Engineering, University of
Plymouth, UK

Sam D. Weller
Senior Research Fellow, University of
Exeter, Penryn Campus, UK

Foreword

Since the 1990s the importance of developing renewable energies has been well recognised worldwide. At the time of writing, onshore wind, solar and hydropower are mature and making relevant contributions to the energy mix. However, the untapped potential of these land-based forms of renewable energy is not unlimited; therefore, new renewable energies, including wave, tidal and offshore wind, must be developed if carbon-based energy production is to be further reduced, in the spirit of the recent Treaty of Paris and previous agreements on climate change.

Offshore wind is technologically more mature than wave and tidal energy, arguably thanks to its similarities with its onshore counterpart. Indeed, as offshore wind moves into deeper waters, those facets that are not shared with onshore wind turbines, such as floating systems or hybrid (wave–wind or tidal–wind) systems warrant the greatest research effort at present.

Wave and tidal energy, the focus of this book, are technologically more challenging, not least because of the aggressive marine environment. Because of this, and the fact that their development began more recently, they are further away from full market commercialisation. Their trajectory has been similar to that of any nascent technology, with initial successes and failures.

Arguably the harsh marine environment has hindered the technological development of both wave and tidal energy, not least in relation to wind energy, the main elements of which were developed for a less aggressive environment. This also made possible the application of wind energy at different scales, from the domestic to the industrial, and its stepwise progression towards the large wind turbines that we see today. Nevertheless, the faster development of wind energy that we have witnessed does not detract in the least from the potential of wave and tidal energy. Given the intensive research efforts and the level of international interest in the field, there can be little doubt that the vast, so far untapped, wave and tidal resource in the ocean will be exploited within the next decades.

This new book aims to provide a reference text for students and practitioners in the wave and tidal energy industry. It presents a holistic view of the sector, the state of the art and the perspectives for future development. The main tools of physical and numerical modelling are explained, together with the technical aspects of device design and development, the environmental effects and the consent and legal processes. These are then illustrated with a series of case studies and a review of regional project developments.

Wave and tidal energy is a fascinating field with many exciting research challenges. Driven by the passion of the researchers and practitioners involved, the momentum in the sector is poised to transform wave and tidal energy from its present research and development status into a fully fledged renewable contributing substantially to the energy mix.

Acknowledgements

This book would not have been possible without the collaboration and wholehearted support of the many authors of the individual chapters. Their expertise in the many facets of wave and tidal energy has been central to the project, and we are greatly indebted to them.

We are grateful to Wiley for suggesting the idea of the book and their consistent support throughout the processes of writing and editing the chapters and producing the book in its final form.

We also acknowledge the contributions and support for this project from the members of the COAST Engineering Research Group and the COAST Laboratory at the University of Plymouth. The Laboratory has been essential to the development of marine renewable energy research at Plymouth. The experience in physical and numerical modelling gained through the activity of the Laboratory and Research Group, working together with industry and academic partners on numerous European and national research and development projects, has resulted in the scientific environment that has ultimately crystallised in this book.

1

Introduction

Deborah Greaves[a] *and Gregorio Iglesias*[b]

[a] *Professor of Ocean Engineering, School of Engineering, University of Plymouth, UK*
[b] *Professor of Coastal Engineering, School of Engineering, University of Plymouth, UK*

1.1 Background

More than 83% of the energy conversion in the world is today based on fossil fuels; meanwhile scientists all over the world are debating the topic of peak oil [1] and the secondary effects of the emissions from the fossil fuels [2, 3]. Fossil fuels are a finite resource; burning them generates significant carbon dioxide emissions that are changing the world's climate. The impact of climate change is thought to be changing habitats at a rate faster than many species can adapt, and the level of pollution in many of the world's cities is today causing concern. As a future worldwide shortage of useful energy supply can have devastating consequences on the political stability and economy of the world, there is a growing consensus that the world needs to switch to a more sustainable energy system. The focus and requirement for clean and cheap renewable energy conversion techniques has therefore increased.

The Paris Summit of 2015 [4] has driven further impetus for finding alternative sources of energy, and a deal was agreed to attempt to limit the rise in global temperatures to less than 2 °C. The Paris agreement is the first to commit all countries to cut carbon emissions, and is partly legally binding and partly voluntary. The measures in the agreement include [5]: to peak greenhouse gas emissions as soon as possible and achieve a balance between sources and sinks of greenhouse gases in the second half of this century; to keep global temperature increase 'well below' 2 °C (3.6 °F) and to pursue efforts to limit it to 1.5 °C; to review progress every 5 years; and $100 billion a year in climate finance for developing countries by 2020, with a commitment to further finance in the future. There is clear acknowledgement of climate change and also a clearly stated will to address the anthropogenic causes of climate change and to reduce emissions and seek alternative sustainable and environmentally benign sources of energy. How this new agreement will be implemented within individual countries will be influenced by local factors.

Renewable sources of energy are essential alternatives to fossil fuels and to nuclear energy, which also has a finite resource as well as long-term safety concerns. Renewable energy sources include solar, wind, geothermal and marine renewable energy (MRE).

Wave and Tidal Energy, First Edition. Edited by Deborah Greaves and Gregorio Iglesias.

Their use reduces greenhouse gas emissions, diversifies energy supply and reduces dependence on unreliable and volatile fossil fuel markets. The world is moving on renewables, and they have become the cornerstone of any low-carbon economy today, not just in the future. The USA is targeting a 32% cut in power sector emissions by 2030, India plans 100 GW of solar by 2022, and China is investing heavily in wind and renewable energy: the transition to a low-carbon energy system is well under way.

Within this drive for renewable energy, MRE is poised to play a major role [6], in particular in certain countries where these resources are vast. Renewable energy from the sea is generated by the sun, wind and tides, and may be exploited through various technologies such as wave energy, tidal stream, tidal range, offshore wind energy and ocean thermal energy currents (OTEC). MRE, also often termed 'ocean energy', has a major part to play in closing the world's energy gap and lowering carbon emissions. Key global challenges that remain for MRE relate to technology, grid infrastructure, cost and investment, environmental impact, and marine governance. Of these technologies, offshore wind is mature and many commercial projects exist in shallow waters, although new offshore wind technology is needed to develop sites further offshore in deeper water. Technologically, the development of offshore wind in shallower water is a natural extension of onshore wind, and typical difficulties for onshore wind in gaining social acceptability and approval are often less problematic if turbines are located offshore. Also, the wind resource offshore is greater due to lack of obstructions to the wind flow. Offshore wind turbines are typically similar to those used onshore and consist of three blades rotating about a hub, and in shallower water the wind turbine structures are typically on piled foundations or fixed jackets. However, as development of wind farms moves further offshore and into deeper water, other solutions need to be sought involving floating structures and the costs increase significantly. Although offshore wind technology is rapidly being implemented, there remain many fascinating engineering problems to overcome. These include: offshore foundations and floating support structures; alternative turbine designs based on three-dimensional computational fluid dynamics; use of advanced materials for blades; ship manoeuvring for safe maintenance; and shared offshore platform applications (such as energy production, storage, and marine aquaculture).

Tidal power is approaching commercial maturity, and recent investments and commercial developments have been made. Tidal range projects exist, but there are concerns about the extent of the environmental impact they bring, and tidal lagoon technology is emerging as an attractive alternative. Tidal steam technologies have seen great advances in recent years. On the other hand, wave energy encompasses emerging technologies that are currently not economically competitive, but still attract engineering interest thanks to the significant resource in high power density sea waves and its potential exploitation [7].

Within Europe, ocean energy is considered to have the potential to be an important component of Europe's renewable energy mix, as part of its longer-term energy strategy. According to the recent studies [8,9], the potential resource of wave and tidal energy is 337 GW of installed capacity by 2050[8] globally, with 36 GW quoted as the practically extractable wave and tidal resource by 2035 in the UK, representing a marine energy industry worth up to £6.1 billion per annum. Today 45% of wave energy companies and 50% of tidal energy companies from the EU [9,10] have been tested in EU test centres [11,12], and the global market is estimated to be worth up to €53 billion annually by 2050 [13].

The need to address climate change and concerns over security of supply has driven European policy-makers to develop and implement a European energy policy. In 2009, the European Commission set ambitious targets for all member states through a directive on the promotion of the use of energy from renewable sources (2009/28/EC). This requires the EU to reach a 20% share of energy from renewable sources by 2020. The directive required member states to submit national renewable energy action plans (NREAPs), that establish pathways for the development of renewable energy sources, to the Commission by June 2010. From their NREAPs, it is clear that many member states predict a significant proportion of their renewable energy mix to come from wave and tidal energy by 2020. This commitment should act as a strong driver at national level to progress the sector.

MRE can significantly contribute to a low-carbon future. Ambitious development targets have been established in the EU, including an installed capacity of 188 GW and 460 GW for ocean (wave and tidal) and offshore wind energy, respectively, by 2050 [10]. To comprehend how challenging these targets are it is sufficient to consider the corresponding targets for 2020: 3.6 GW and 40 GW for ocean and offshore wind energy, respectively. It is clear that for the 2050 targets to be met, a major breakthrough must happen – and there are huge benefits to be reaped if these targets are met, such as the reduction of our carbon footprint.

1.2 History of Wave and Tidal Energy

Although MRE and ocean energy can be interpreted to include all energy conversion technologies located in the ocean environment, including offshore wind, OTEC as well as wave and tidal, in this book we focus on wave and tidal energy. Tidal energy converts the energy obtained from tides into useful forms of power, mainly electricity. Tides are more predictable than wind energy and solar power. Among the sources of renewable energy, tidal power has traditionally suffered from relatively high cost and limited availability of sites with sufficiently high tidal ranges or flow velocities, thus constricting its total availability. However, significant learning has been gained through relatively long-term deployments of tidal turbines [14], and together with developments in tidal lagoon technology [15], and first array scale deployments [16], it is expected that the total availability of tidal power is significant, and that economic and environmental costs may be brought down to competitive levels.

Historically, tide mills [17] have been used both in Europe and on the Atlantic coast of North America for milling grain, and in the nineteenth century the use of hydropower to create electricity was introduced in the USA and Europe [18]. Tidal range projects include the world's first large-scale tidal power plant, the La Rance Tidal Power Station in France, which became operational in 1966 [19]. It was the largest tidal power station in terms of power output, before Sihwa Lake Tidal Power Station in South Korea (described in Chapter 12) surpassed it. Many innovative tidal stream energy devices have been proposed. An example is Salter's cross-flow turbine [20], which has blades arranged vertically, supported at each end on what are rather like enormous bicycle wheels. Although tidal power assessment seems easy, the very presence of tidal turbines alters the flow field, and in turn this affects power availability.

Tidal energy technology is dominated by in-sea/estuarine tidal stream devices; however, a significant number of developers have also been developing smaller in-river devices.

There is certainly potential for tidal energy to consolidate technologies and progress from small-scale to larger developments within the full-scale prototype field. The last few years to 2016 have seen the total number of globally active developers fall, perhaps as the technology naturally converges. Leading developers are actively testing at EMEC [21] and moving strongly towards commercial readiness and preparing for transition to large-scale commercial generation in the UK Crown Estate lease areas, north-west France and Canada's Bay of Fundy. Alongside the progress to full-scale device deployment technology activity, there has been clear progress on site development, with the consent and finance secured for a 6 MW tidal array off the north of Scotland by MeyGen and the subsequent news of Atlantis Resources Ltd. having purchased the project. This is the first example of real value being attributed to a site and associated development consent [22].

The Severn Estuary holds the second highest tidal range in the world, and within this Swansea Bay benefits from an average tidal range during spring tides of 8.5 m. Plans to construct a tidal lagoon [15] to harness this natural resource would be the world's first, man-made, energy-generating lagoon, with an expected 320 MW installed capacity and 14 hours of reliable generation every day. In a bid to overcome potential socio-economic and environmental concerns, the development also offers community and tourism opportunities in sports, recreation, education, arts and culture, conservation, restocking and biodiversity programmes as well as the added benefit of coastal flood protection.

Wave energy converter technology is a thriving area in which new inventions keep appearing. Here, engineers must find ways to maximise power output, improve efficiency, cut environmental impact, enhance material robustness and durability, reduce costs, and ensure survivability. Theoretical predictions of the power generated by wave energy converters require validation through laboratory-scale physical model studies and field tests. The latest simulation methods involve wave to wire modelling of arrays of wave energy converters, which integrates wave hydrodynamics, body responses, power take-off (PTO), real-time control, and electricity production.

There are more than one thousand patents for devices for capturing and transforming wave energy into useful energy. The first wave energy converter was patented in France in 1799, and oscillating water column navigation buoys have been commercialised in Japan since 1965 [6]. The oil crisis in 1973 raised interest in wave energy in Europe, but interest dwindled in 1980s and it was not until the 1990s that interest increased again.

Wave energy has the largest potential in Europe and worldwide, and can be captured in a number of ways through the use of different converters, such as point absorbers, attenuators, overtopping, oscillating wave surge convertors, and oscillating water columns. The technology has not yet reached the stage of commercial scale development [23], but progress continues to be made, as evidenced by the growing number of test sites and pilot zones being established across Europe [11]. Many different types of wave energy converters have been designed, but only a small proportion of these so far have reached the full-scale prototype stage. Wave energy has many advantages over other forms of renewable energy, being much more predictable than, for instance, wind, giving more scope for short-term planning of grid usage.

In the past, the wave energy industry faced some failures that delayed its development, for example the device in Toftestallen wrecked during a heavy storm [24] or the external wall of the Mutriku device that was damaged by a storm [25]. Attempting to set a framework for assessing the progress of potential developers on their way to commercial applications, Weber [26] introduced the technology readiness level and technology performance level matrix, so that fewer failures occur in the future.

1.3 Unknowns and Challenges Remaining for Wave and Tidal Energy

Access to ocean energy systems is expensive and hazardous. Present and future challenges include remote monitoring, control systems, robotics for operational support, and real-time weather forecasting for predictive maintenance to ensure devices can survive in extreme sea states as they arise. Wave and tidal energy has huge potential, but demanding global challenges have to be met before the seascape will give up its precious energy resources. As in the Industrial Revolution, a new generation of engineers is required with the ingenuity, wisdom, and boldness to meet these interdisciplinary challenges. The unknowns and challenges still remaining in wave and tidal energy can be considered to fall within ten different technical research themes as identified by PRIMaRE [27]: materials and manufacture; fluid dynamics and hydrodynamics; survivability and reliability; environmental resources; devices and arrays; power conversion and control; infrastructure and grid connection; marine operations and maritime safety; socio-economic implications; and marine planning and governance.

1.3.1 Materials and Manufacture

The development of new materials and manufacturing processes is a key element in reducing costs and ensuring the survivability of MRE devices. Any technology submerged or in contact with the sea is likely to be affected by biofouling. The interaction of the devices or their components with marine growth is crucial as it affects the device performance and design conditions, and therefore the development of new materials to avoid or minimise biofouling is key. Use of steel or metallic alloys is common practice in the MRE industry. Correct understanding of the corrosion processes, of the use of new coatings and manufacture techniques, and of how to adapt the operation and maintenance inspections to maximise the lifetime and operability of MRE devices will help reduce their total cost. Application of novel materials and construction techniques that will reduce costs, improve reliability and extend the lifetime of devices is an active research area, necessary to move the sector forward – for example, novel materials such as reinforced concrete and composites, novel construction techniques, disposable materials are being investigated.

1.3.2 Fluid Dynamics and Hydrodynamics

As technology devices that harness energy from fluids in motion and are affected by the extreme forces produced by these motions, a proper understanding of the fluid dynamics and hydrodynamics of MRE devices is crucial to their development. In particular, turbulence and its effects on single and multiple devices is important in understanding how devices will interact and perform in arrays. In the real sea environment MRE devices commonly face the effects of combined waves, tidal currents and wind. The combined action of these forces on MRE devices makes characterisation of their response at laboratory scale and with numerical models of special relevance to obtain a better understanding of how they perform under such circumstances. One of the particularities of MRE is that the devices need to face extreme loads and survive storms. Thus, the development of novel evaluation techniques to model these extreme loads appropriately at laboratory scale and by numerical models is required.

When deployed in real sea conditions, MRE devices are subjected to irregular waves and variable tidal currents. A feature of these variable resources is that the differences between maximum and mean values are particularly high, especially for wave energy. The standard engineering techniques to model the behaviour and response of MRE devices consider linear models in order to simplify the problems and obtain faster solutions. However, the reality is often far from the linear model and nonlinear effects must be considered to achieve a proper understanding of the performance of the devices in real conditions. Thus, the development of nonlinear models and tools to assess these effects is of special relevance. Advanced numerical models able to simulate accurately the response of full-scale devices require long computational times and resources. The development of validated tools and resources that optimise simulation times is necessary for the development of MRE.

1.3.3 Survivability and Reliability

The survivability and reliability of MRE devices in the marine environment need to be proven for the industry to become commercial. Ensuring the survivability of devices under the high loads occurring during extreme events is essential to reduce the risk of failure and increase their range of operability. The dynamic nature of many MRE devices means that traditional oil and gas or seakeeping mooring concepts are usually not valid, due to either their high cost or the different loading conditions. A competitive cost of energy which allows MRE to become viable in comparison with other renewable energies is fundamental for the development of the sector. This means that a compromise between reliability and cost of energy throughout the lifetime of the device should be found. The weakest of its components defines the entire reliability of a MRE device. This, together with the harshness of the marine environment, the frequent exposure to extreme loads, and near-constant exposure to varying cyclic loads, makes the design of all components crucial. Research is needed to assess each individual component and adapt it to the MRE industry needs, redesigning components where necessary and making use of available technology where possible, for example from the oil and gas sector. Furthermore, MRE devices are subject to potential impacts, for example, the impact of a marine mammal striking the rotor of a tidal turbine, or collision between wave energy converters due to a mooring failure, and these impacts could severely damage the integrity of the device.

1.3.4 Environmental Resources

Resource assessment for wave and tidal energy is described in Chapter 2, and a thorough understanding of the environmental resources is imperative to harnessing them in an economic and efficient manner. Even though wave, tidal currents and offshore winds are well understood at medium and large scales, there are still multiple physical processes related to them that require further study, especially when energy extraction is involved: turbulence, atmospheric thermal gradient, oceanic fronts, salinity, spatial (and spectral) variability of waves, sediment transport, etc. Wave, tidal and wind macro-scale models are well known and have been validated in recent years [28,29]; however, to transfer the input from these large-scale models to more reduced-scale regional models still requires further research [30]. Monitoring MRE resources at the sea is expensive and sometimes risky or impossible due to the weather conditions. The development of novel remote sensing techniques which allow monitoring of MRE resources further from the site or to cover larger areas will help to reduce uncertainties about the resource and its costs, such as floating LIDARs, high-frequency radars [31], and satellite monitoring. Forecasting MRE resources with high resolution is important not only to be able to predict the energy production, but also to inform control strategies that require being able to predict and respond precisely to the incoming resource.

1.3.5 Devices and Arrays

The level of technological development among MREs is very variable, depending on the type of energy being harnessed; thus on the one hand floating offshore wind and tidal turbines have successfully achieved full-scale demonstrations and are moving towards arrays, while on the other hand wave energy converters are less developed in their progression towards array deployments. Accessibility of MRE devices at sea is not always possible due to the weather conditions, and therefore developing remote monitoring and control techniques and operation procedures becomes an important requirement to increase operation times and reduce operation & maintenance (O&M) costs. Mooring systems for MRE devices are a crucial subsystem that influences both the global performance of the device and its survivability. However, for arrays of MRE devices, and in particular interconnected arrays, these become even more important because the layout of the array will be highly dependent on the mooring dynamics and interactions. Few MRE devices have been tested in arrays so far, which means that significant unknowns remain around how the energy extraction of some devices will affect the performance of the other devices in the array. This is an important research topic as it will influence significantly the layout of future arrays. One aspect of arrays is that they may lead to sharing of some infrastructure, such as the mooring lines and PTO, with the consequent cost reduction. Future research is needed in order to assess whether sharing of these subsystems is appropriate or not [32].

1.3.6 Power Conversion and Control

Ultimately MRE devices are meant to produce electricity at an affordable cost. This means that power conversion and control subsystems are fundamental parts of an MRE device. A PTO is a key component of every MRE device, as it is through this that the power is ultimately harnessed. Increasing the performance of PTOs, making them more reliable and extending their lifetime are required steps to reduce MRE costs. Due to the irregular character of MRE resources, and in particular of wave energy, control strategies are required in order to maximise the power output. At present the relatively high cost of MRE, together with the high variability in power production, means that additional research is needed to tackle these issues. Novel power electronics control systems able to transform the variable energy production obtained from the MRE resources into conditions required for the electric grid may be part of the solution and are required for successful development of the devices.

1.3.7 Infrastructure and Grid Connection

For offshore energy projects, the infrastructure and grid connection costs represent one of the largest components of the total project costs. The development of novel concepts of subsea electric connectors which will allow reduced times for installation, decommissioning and standard plug and unplug operations during O&M is required. The development of specific protocols and tools for O&M procedures at MRE test centres is of special interest in order to extrapolate them to other future projects. Furthermore, these test centres can also be used to develop and test novel O&M techniques. The combination of more than one MRE technology at the same site is a novel approach that takes advantage of the multiple synergies arising from deployment of more than one technology at the same location. Understanding the implications of this practice is crucial in order to further develop these kinds of projects. Integrating the energy harnessed at MRE parks into the energy grid is not a simple task due to the existence of multiple challenges, such as the lack of grid infrastructure inland near the parks, the variable character of the energy production, and the lack of coupling between the production of and the demand for energy.

1.3.8 Marine Operations and Maritime Safety

Operations and safety at sea are not simple due to the variable conditions and harsh working environment, which means that operations to access an offshore device or to deploy a wind turbine may be high-risk challenges. Further research in order to simplify and reduce the risk in these tasks is crucial to further develop the sector. The consideration of the decommissioning phase of a MRE device at its development phase is very relevant in order to save time and resources. Further research is needed in order to include these aspects during the development phase or the design of novel materials or devices. To access an offshore device is not a simple task, especially when the sea conditions differ. This means that at some sites device access times are reduced to below 60% of the year, resulting in an increase in O&M costs and in performance reduction. Design of novel access techniques or unmanned O&M protocols is one of the main challenges for the MRE sector to accomplish in order to reduce operation costs. The deployment of more than one MRE technology at the same site has the associated risk of possible interference between technologies (e.g., reducing the energy production, collision or impact between devices). In order to make this promising solution a reality, these challenges must be further addressed in the coming years. An accurate forecast of the weather windows to access offshore sites to perform O&M and deployment activities is highly important to reduce costs and deployment times. Future research is needed in order to produce new short- and long-term models to forecast weather windows.

1.3.9 Socio-Economic Implications

As MRE develops beyond the demonstration scale, improved knowledge of the potential socio-economic implications of larger arrays is required. In particular, a better understanding is needed of the social, economic and environmental costs and benefits and how they are distributed spatially and temporally between local, regional and national levels. The findings of this empirical research can then be applied to support marine planning, licensing, and governance and stakeholder engagement.

The foundation for understanding socio-economic issues is to determine how stakeholders and the wider public perceive the development and impacts of MRE, and which socio-demographic factors shape their attitudes. At present, the public has very limited awareness of MRE, and it is therefore important to understand how different messages and media types are perceived as sources of credible information. There is a growing policy trend to seek to understand environmental impacts in terms of their societal implications, which is achieved through the framework of ecosystem services. Ecosystem service approaches also facilitate monetary valuation of natural capital impacts, and hence support enhanced cost–benefit analysis of MRE developments and natural capital accounting. For these reasons, ecosystem service approaches need to be embedded in full life-cycle analysis of MRE.

Commercial-scale MRE developments have the potential to bring economic benefits through, for example, job creation and supply chain development, although other sectors (fisheries, recreation) may be negatively affected. At present, the scale of these effects and their implications for regional and national economies are poorly understood. Also key to planning and policy decisions is understanding how the benefits of MRE development, such as clean, renewable energy and job creation, are traded off against natural capital and ecosystem service impacts at the level of individual energy consumers, local communities, and regional and national economies.

Traditionally the marine and maritime sectors have been characterised by the absence of coordinated planning and governance, as opposed to what happens onshore, where coordinated regulations and planning have been in place for many years (e.g., land use planning, mining exploitation concessions and natural protected areas). However, in recent years some EU initiatives, such the Maritime Policy, Maritime Spatial Planning, Integrated Coastal Protection Management, Marine Strategy Framework and Water Framework Directives (via consideration of impacts of MRE on the targets of good environmental/ecological status), are driving the need for more coordinated planning of the marine and coastal space. Integration of the uses of different resources is key to ensuring sustainable development.

The engagement of stakeholders and especially local communities is an important aspect of the successful development of an MRE project. Many examples show that disregarding these actors at early stages of project development has been damaging for the projects. Developing novel tools to facilitate this engagement and to increase the communication between developers and stakeholders is of special relevance for the success of future MRE projects. An appropriate assessment and planning of the complete life cycle of an MRE device is important to increase the sustainability of the technology. The development of new generation concepts and new tools to tackle this at full scale is necessary.

1.3.10 Marine Planning and Governance, Environmental Impact

Appropriate planning of the spatial distribution of maritime resources and uses is vital for sustainable development of the seas and its coexistence with traditional and new users. Significant effort has been made by European and national administrations to start this large endeavour; however, future research is needed to propose novel approaches to planning and managing use of the sea's resources. Multiple marine resources are usually available at the same site or geographical location, and synergies between the different users of these resources exist. Sustainable development of the exploitation requires multi-use of these marine resources, for which further research and development to prove its viability is needed. Research and demonstration of the options for combinations of wave and offshore wind energy with other uses, such as aquaculture or maritime leisure, is required for successful implementation of multi-use of space.

Understanding the effects on the physical coastal processes of the deployment of MRE infrastructure, such as mooring anchors and solid foundations, is of special relevance to understanding how these technologies affect the environment. Energy extraction from harnessing waves or tidal currents affects the wave and flow field and sediment transport processes occurring in them. This may have a significant effect on coastal erosion phenomena for large and cumulative scale effects of MRE deployments. The interaction between solid foundations of MRE devices and currents and waves produces erosion of the seabed in the surroundings of the structure. Known as 'scour', this phenomenon may alter the baseline sediment transport processes, and further research is needed in order to understand the significance of this effect. There is a lack of international standards or common industry practice concerning the required burying depth for electrical marine cables, and the effects of the electromagnetic fields over the ecosystem are not well understood [33].

The deployment of MRE devices inevitably involves contact with the seabed and so has a clear effect on the benthic flora and fauna. The presence of new structures altering the environment could potentially act as barriers or generate displacements or migrations in benthic communities. In order to understand these possible effects further research should be conducted during future deployments of MRE devices. The energy extraction caused by harnessing marine resources could potentially affect the trophic chain, and the presence of MRE devices could affect the production of nutrients, displace species, etc. Deploying MRE devices creates new habitat with a potential risk of introducing non-native invasive species that can significantly alter the ecosystem. New research should be conducted to understand this risk and develop contingency measures to avoid it.

In addition to the research needs for the benthic communities, there are others that affect local communities such as fishes, birds and marine mammals. Development of novel active and passive acoustic monitoring techniques and instruments is an important area of research needed to acquire a better understanding of how MRE devices affect local communities. As MRE device deployment continues, the study of such interactions using novel techniques and the development of new instrumentation will be of particular relevance (e.g., new hydrophones or lateral sonars able to record the interaction of local communities with MRE devices). Modelling the behaviour of marine mammals, as individuals in the upper levels of food chains and of societal importance, is also needed to understand possible effects of MRE devices and so that accurate behaviour models for marine mammals may be developed.

One of the possible positive impacts of deploying MRE devices is the creation of artificial reefs; however, this needs to be monitored in order to fully understand the effects. In order to do this, new research including monitoring of new deployments of MRE devices and the use of computer models is needed. Large individuals such as marine mammals may be at risk of collision or entanglement with the MRE devices or some of their subsystems (e.g., impact of a marine mammal with a tidal turbine or entanglement with mooring lines). The development of models incorporating behavioural characteristics of marine mammals is needed to assess and simulate their response to MRE developments.

In summary, MREs are among the renewables with the greatest potential; however, to succeed in the quest to develop the MRE energy sector, some significant challenges need to be tackled in the coming years. Wave and tidal energy provide an unlimited 'clean' resource from which to generate electrical power and thus make a significant contribution to the renewables mix. Realisation of this potential, however, will require continuing advances in marine engineering technology in order to achieve economic viability and ensure minimal environmental impact.

1.4 Synopsis

The aim of this book is to establish an authoritative, up-to-date reference text that will assist advanced study and research in wave and tidal current energy to maintain progress in the field. In Chapter 2, the marine resource is described, including wave and tidal energy resource assessment, a discussion of the alternative approaches, and acknowledgement that there is still some lack of consensus on resource assessment, while making informed recommendations on methodology, *in situ* measurement and data analysis techniques.

In the next two chapters, the fundamentals of wave and tidal technology are given. In Chapter 3 wave energy converter (WEC) technology is described, and the fundamental theory, the history of development and the categorisation of WECs are discussed. Tidal energy technologies described in Chapter 4 include horizontal and vertical axis turbines; the chapter also covers both tidal stream and tidal lagoon technologies.

Device design is tackled in Chapter 5, in which the development and application of standards is described together with structural design, moorings and reliability. The power systems developed for wave and tidal energy are explored in Chapter 6, and theory is given for power take-off and control.

Key components of the design and development of any MRE system are physical and numerical modelling. In Chapter 7, scale model testing of single devices and arrays in laboratory facilities and larger-scale device testing at sea are described. Testing protocols are also discussed, as well as the different scales appropriate for different stages of design. Chapter 8 gives a thorough overview of numerical modelling for wave and tidal energy. It includes a discussion of the role of numerical modelling in the design process, a brief discussion of the numerical models available, their governing equations and their use within MRE. These include resource models, device design models, farm design models (energy yield and environmental impact), power train models (and control).

In order for a wave or tidal project to be realised, the potential environmental impacts need to be considered and mitigated if appropriate. Chapter 9 describes environmental impact assessment for both physical and biological systems. Each aspect includes a detailed discussion on the near-field and far-field effects of arrays, the short- and long-term impacts, as well as impact assessment and monitoring techniques.

Consenting and legal aspects of wave and tidal energy development are considered in Chapter 10, with a discussion of consenting processes and marine planning procedures, national perspectives and of experience gained from MRE consenting processes.

In Chapter 11, the economics of wave and tidal energy is covered, including the levelised cost of energy approach and the externalities – an important aspect which, if applied to the different energy sources, can contribute to the implementation of optimal electricity production and prices. In Chapter 12, the different stages of project development are illustrated through four representative case studies: two in tidal energy and two in wave energy. With a structure articulated around these case studies, Chapter 12 brings together device design, array planning, policy and economics, drawing material from other chapters, and including detailed discussions of technical aspects (e.g., access and deployment strategies, installation, and reliability and maintenance) and non-technical aspects (e.g., planning, consenting, economic assessment and externalities, financing).

Chapter 13 gives an up-to-date review of developments worldwide, covering regional activities in Europe, North America, Latin and Central America, Asia-Pacific and China. The book concludes with an epilogue on the future of wave and tidal energy.

References

1 Kharecha, P. and Hansen, J. (2008) Implications of 'peak oil' for atmospheric CO_2 and climate. *Global Biogeochemical Cycles* 22(3), GB3012.

2 Nel, W.P. and Cooper, C.J. (2009) Implications of fossil fuel constraints on economic growth and global warming. *Energy Policy* 37(1), 166–180.

3 Pacala, S. and Socolow, R. (2004) Stabilization wedges: Solving the climate problem for the next 50 years with current technologies. *Science* 305(5686), 968–972.

4 Willis, R. (2015) Paris 2015: getting a global agreement on climate change. http://www.green-alliance.org.uk/resources/Paris

5 http://www.theguardian.com/environment/2015/dec/12/paris-climate-deal-key-points

6 Clément, A., McCullen, P., Falcão, A., Fiorentino, A., Gardner, F., Hammarlund, K., Lemonis, G., Lewis, T., Nielsen, K., Petroncini, S., Pontes, M.-T., Schild, P., Sjöstrom, B.-O.; Sørensen, H.C. and Thorpe, T. (2002) Wave energy in Europe: Current status and perspectives. *Renewable and Sustainable Energy Reviews* 6(5), 405–431.

7 Enferad, E. and Nazarpour, D. (2013) Implementing double fed induction generator for converting ocean wave power to electrical. *4th Power Electronics, Drive Systems and Technologies Conference (PEDSTC)*. Piscataway, NJ: IEEE.

8 IEA-Ocean Energy Systems, Annual Report 2013. https://www.ocean-energy-systems.org/documents/82577_oes_annual_report_2013.pdf

9 Magagna, D. and Uihlein, A. (2015) Ocean energy development in Europe: Current status and future perspectives. *International Journal of Marine Energy* 11, 84–104.

10 JRC (2015) *2014 Ocean Energy Status Report*. European Commission. https://setis.ec.europa.eu/sites/default/files/reports/2014-JRC-Ocean-Energy-Status-Report.pdf

11 Osta Mora-Figueria, V., Huerta Olivares, C., Holmes, B., O'Hagan, A.M., Torre-Enciso, Y. and Leeney, R.H. (2011) Catalogue of Wave Energy Test Centres, Plymouth. https://www.plymouth.ac.uk/research/coast-engineering-research-group/sowfia-project.

12 O'Callaghan, J., O'Hagan, A.M., Holmes, B., Muñoz Arjona, E., Huertas Olivares, C., Magagna, D., Bailey, I., Greaves, D., Embling, C., Witt, M., Godley, B., Simas, T., Torre Enciso, Y. and Marina, D. SOWFIA Work Package 2 Final Report. https://www.plymouth.ac.uk/research/coast-engineering-research-group/sowfia-project.

13 House of Commons Energy and Climate Change Committee (2012) *The Future of Marine Renewables in the UK. Government Response to the Committee's Eleventh Report of Session 2010–12*. London: The Stationery Office. http://www.publications.parliament.uk/pa/cm201213/cmselect/cmenergy/93/93.pdf

14 Douglas, C.A., Harrison, G.P. and Chick, J.P. (2008) Life cycle assessment of the SeaGen marine current turbine. *Proceedings of the Institution of Mechanical Engineers, Part M: Journal of Engineering for the Maritime Environment* 222(1), 1–12.

15 Baker, C. and Leach, P. (2006) *Tidal lagoon Power Generation Scheme in Swansea Bay: A Report on Behalf of the Department of Trade and Industry and the Welsh Development Agency*. London: DTI.

16 Lewis, M., Neill, S.P., Robins, P.E. and Hashemi, M.R. (2015) Resource assessment for future generations of tidal-stream energy arrays. *Energy* 83, 403–415.

17 Minchinton, W.E. (1979) Early tide mills: Some problems. *Technology and Culture* 20(4), 777–786.

18 Dorf, R. (1981) *The Energy Factbook*. New York: McGraw-Hill.

19 Andre, H. (1978) Ten years of experience at the 'La Rance' tidal power plant. *Ocean Management* 4(2), 165–178.

20 Salter, S.H. (2012) Are nearly all tidal stream turbine designs wrong? Paper presented to 4th International Conference on Ocean Engineering.

21 www.emec.org.uk, accessed 20/01/2016

22 Marine Energy Global Technology Review 2015. http://www.marine-energy-matters.com/globaltechnologyreview2015, accessed 06/09/2017

23 Strategic Initiative for Ocean Energy (SI OCEAN) https://ec.europa.eu/energy/intelligent/projects/en/projects/si-ocean, accessed 19/01/2016

24 Charlier, R.H., Chaineux, M-C.P., Finkl, C.W. and Thys, A.C. (2010) Belgica's Antarctic toponymic legacy.' *Journal of Coastal Research* 26(6), 1168–1171.

25 Torre-Enciso, Y., Marqués, J. and López de Aguileta, L.I. (2010) Mutriku. Lessons learnt. In *Proceedings of the 3rd International Conference on Ocean Energy*.

26 Weber, Jochem. "WEC Technology Readiness and Performance Matrix–finding the best research technology development trajectory." *International Conference on Ocean Energy*. 2012.

27 www.Primare.org, accessed 19/01/2016.

28 van Nieuwkoop, J.C., Smith, H.C., Smith, G.H. and Johanning, L. (2013). Wave resource assessment along the Cornish coast (UK) from a 23-year hindcast dataset validated against buoy measurements. *Renewable Energy* 58, 1–14.

29 Blunden, L.S. and Bahaj, A.S. (2007). Tidal energy resource assessment for tidal stream generators. *Proceedings of the Institution of Mechanical Engineers, Part A: Journal of Power and Energy*, 221(2), 137–146.

30 Roc, T., Conley, D.C. and Greaves, D. (2013) Methodology for tidal turbine representation in ocean circulation model. *Renewable Energy* 51, 448–464.

31 Lopez, G., Conley, D., and Greaves, D. (2015) Calibration, validation and analysis of an empirical algorithm for the retrieval of wave spectra from HF radar sea-echo. *Journal of Atmospheric and Oceanic Technology* 33(2), 245–261.

32 WETFEET H2020 Project (2014) http://www.wetfeet.eu/, accessed 19/01/2016.

33 Greaves, D., Conley, D., Magagna, D., Aires, E., Chambel Leitão, J., Witt, M., Embling, C.B., Godley, B.J., Bicknell, A., Saulnier,J-B., Simas, T., O'Hagan, A.M., O'Callaghan, J., Holmes, B., Sundberg, J., Torre-Enciso,Y. and Marina, D., (2016) Environmental Impact Assessment: Gathering experience at wave energy test centres in Europe. *International Journal of Marine Energy* 14, 68–79.

2

The Marine Resource

Gregorio Iglesias

Professor of Coastal Engineering, School of Engineering, University of Plymouth, UK

2.1 Introduction

This chapter is concerned with the characterisation of the energy resource from wind waves and tides – a fundamental step towards its exploitation. The term 'characterisation' goes beyond a mere assessment of the resource, and implies an in-depth analysis of its characteristics [1]. For instance, in the case of the wave resource, it is not sufficient to state that the mean wave power at a given site in an average year is 50 kW m^{-1}; this overall figure, for all its interest, must be complemented with the analysis of the characteristic parameters of the sea states providing the energy: their significant wave heights, energy periods, mean wave directions, etc. This information is essential in determining the actual power output that can be obtained from a particular Wave Energy Converter (WEC), as well as I selecting the WECs that are best suited to the characteristics of the wave resource at the site in question [2]. The wave and tidal resources are covered in Sections 2.2 and 2.3, respectively.

2.2 The Wave Resource

Wind waves, infragravity waves, tsunamis, tides, etc. – there exist many types of waves in the ocean, with different driving mechanisms and properties. However, the term *wave energy* does not refer – at least in its common usage – to all of them, but to a particular type of waves: wind waves, those generated by the wind blowing over the sea [3]. Winds are ultimately the result of solar energy acting on the atmosphere, and therefore wave energy may be regarded as a concentrated form of solar energy – and the oceans, as a gigantic energy conversion system transforming one type of mechanical energy (wind energy) into another, more concentrated type (wave energy).

Considering that the oceans cover 71% of the Earth's surface and that wind waves can propagate over long distances with little energy loss, it is not surprising that a substantial amount of wave power reaches almost continuously any stretch of coastline open to the ocean. This quasi-ubiquity of wave power inshore constitutes one of its principal

Wave and Tidal Energy, First Edition. Edited by Deborah Greaves and Gregorio Iglesias.

advantages, and explains the enormous, virtually unlimited global resource – which has been estimated at 32,000 TWh per year [4].

Indeed, wave energy has great potential for development, and its present status is reminiscent of wind energy in the 1980s. The deployment of arrays of WECs, also known as *wave farms*, to harness this vast, untapped resource is hindered by a number of factors, not least the lack of maturity of the technology and the concomitant high costs, which curtail the competitiveness of wave energy *vis-à-vis* other renewables. For wave energy to truly take off, development on four fronts is necessary. First, robust and efficient WECs must be developed (e.g. [5–8]). Second, the resource must be thoroughly characterised so that the areas of interest can be selected and the energy output of prospective wave farms determined [1, 4, 9–13]). Third, the economics of these farms must be assessed, which requires – in addition to the characterisation of the resource – a thorough understanding of the lifetime costs of the WECs themselves and the other components of a wave farm, including their installation, maintenance and decommissioning, as well as the balancing costs of accommodating a fluctuating power source into the network [14–17]. The cost of wave energy may be reduced by realising synergies with other renewables, most notably wind energy [18–24]. Finally, the impacts of wave energy on marine and, in particular, coastal environments must be assessed at different time scales, from the short to the long term; in fact, some of these impacts may turn out to be positive – in the form of a reduction in the amount of wave energy reaching vulnerable coastlines, and research is under way on the application of wave farms to coastal erosion management in synergy with their primary purpose, carbon-free energy generation [25–29].

The motivation for characterising the wave resource is clearly practical, with a view to its exploitation by means of wave farms; these must be situated near the coastline – in some cases, *on* the coastline[1] – for reasons to do with economic viability. Indeed, a number of relevant costs spiral with increasing distance to the coastline and water depth, including those of the submarine cable, mooring system, and maintenance. However, there are also advantages to locating the farm some distance from the shoreline, such as avoiding the harsh environment of the surf zone (a practical necessity, for breaking waves would compromise the survival of the WECs), reducing the visual impact from the coast and, generally speaking, tapping into a greater resource. All these factors must be pondered locally, for each project, and a compromise struck. In principle it may be assumed that wave farms will not be deployed in water depths above 100–150 m, and will consist primarily of floating WECs – bottom-fixed alternatives being too expensive; therefore, it is the *nearshore* wave resource that we are primarily interested in.

Generally speaking, the nearshore wave resource is less uniform than its offshore counterpart, the reason being that waves do not interact with the seabed in deep water. Ocean waves propagate over deep water until, eventually, they approach a coast. When the water depth decreases to half the wavelength, i.e. when the relative water depth, h/L, is ½ (with h the water depth and L the wavelength), the wave begins to interact with the seabed and, by definition, leaves deep water to enter transitional water. To visualise this it is useful to consider the concept of *wave base* – a reference horizontal plane at a depth

1 Onshore WECs are indeed a possibility, and may be of interest in particular cases, for instance mounted on (new) coastal structures, as in Mutriku (Spain), but it is doubtful that they will ever be deployed in numbers large enough to provide substantial power, not least because of the impact that this would have on coastal landscapes.

of a half wavelength, $L/2$, beneath which the effects of the wave on the water column (orbital motions of the water particles, pressure fluctuations, etc.) are negligible.[2] In other words, for all practical purposes the wave extends vertically from the surface to the wave base. In deep water, the wave base is above the seabed, implying that there can be no interaction between the wave and the seabed. At some point in the wave propagation towards the coast, the water depth becomes equal to, then smaller than, $L/2$; from that point onwards the wave is constrained vertically by the seabed, and this will affect its properties. That point marks the end of deep water and the beginning of transitional water – an altogether different regime in which the *phase celerity* (the speed at which the wave propagates) is determined no longer by the wave period alone but also by the water depth.[3] We shall see below that this all-important control of the phase celerity by the water depth and the wave period is governed by the dispersion relationship. In essence, as the properties of the medium (water depth) through which the wave propagates change, so does the propagation velocity. This change in the phase celerity causes a change in the direction of propagation – a process known as *refraction*, which, incidentally, affects not only waves in the ocean but also other types of waves, and even light. In the case of ocean waves, the change in the direction of propagation leads to changes in wave height, power, etc. Furthermore, as the wave travels over transitional water the varying water depths lead to changes in the *group celerity* (the speed at which wave *energy* propagates), which in turn also lead to changes in wave height, power, etc. – a process known as *shoaling*. In sum, in transitional water varying water depths affect the fundamental wave parameters (with the exception of the wave period, nonlinearities excluded). As a result of refraction and shoaling, and other processes such as friction with the seabed, the relative uniformity of the wave field in deep water is gradually transformed into ever greater spatial variability – in particular, where the bathymetry (the seabed contours) is highly irregular.

We have seen why the nearshore wave resource presents significant spatial variability. Whereas certain areas – the *nearshore hotspots* [30] – have a substantial resource, nearby areas have a much lower resource. This spatial variability is a crucial element that must be accounted for in the characterisation of the resource and, particularly, in the selection of prospective wave farm sites [31]. Similarly, the temporal variability must be considered, for it will determine the performance and energy output of the wave farm, as well as the survivability of its WECs [2, 31–34]. For these reasons, a thorough characterisation of the spatial and temporal variability of the nearshore wave resource in the area of interest is a prerequisite to assessing the economic viability of a wave farm project [14, 16].

A brief note on the structure and contents of this section. Ideally, the reader should be familiar with wave theory before delving into the characterisation of the wave resource; a brief summary of the theory is presented in Sections 2.2.1 (linear wave theory) and

2 This value of $L/2$ is admittedly somewhat arbitrary, and related to the interpretation, or quantification, of "negligible"; strictly speaking, the effects of the wave on the water column (orbital motions of water particles, pressure fluctuations, etc.) decrease exponentially with water depth and therefore do not become zero at any finite depth, but tend to zero at infinity.

3 Later on, as the wave continues to propagate towards the coast, a second threshold of relative water depth, $h/L = 1/20$, will eventually be reached, marking the end of transitional water and the beginning of shallow water – yet a different regime in which waves cease to be dispersive, that is, the phase celerity is controlled exclusively by the water depth.

2.2.2. (random waves). The characterisation of the wave resource proper is covered in Sections 2.2.3 (offshore resource) and 2.2.4 (nearshore resource).

2.2.1 Fundamentals of Linear Wave Theory

In linear wave theory, also known as Airy wave theory, the displacement of the free surface (the sea surface) is given by

$$\eta = \frac{H}{2}\cos\left(\frac{2\pi}{L}x - \frac{2\pi}{T}t\right), \tag{2.1}$$

where η is the vertical excursion of the free surface, H is the wave height, L the wavelength, and T the wave period. If the amplitude, wavenumber and angular frequency are denoted by a, k and ω, respectively, then

$$a = \frac{H}{2}, \tag{2.2}$$

$$k = \frac{2\pi}{L}, \tag{2.3}$$

$$\omega = \frac{2\pi}{T}, \tag{2.4}$$

and the sinusoidal displacement of the free surface, equation (2.1), may be rewritten as

$$\eta = a\cos\left(kx - \omega t\right). \tag{2.5}$$

The wavenumber, angular frequency and water depth (h) are related through the dispersion relationship,

$$\omega = kg\tanh\left(kh\right), \tag{2.6}$$

with g the gravitational acceleration. Alternatively, the dispersion relationship may be expressed in terms of the wavelength, period and water depth:

$$L = \frac{gT^2}{2\pi}\tanh\left(\frac{2\pi h}{L}\right). \tag{2.7}$$

Of importance here is the fact that, for a given wave period at a certain point (water depth), there exists only one wavelength that satisfies equation (2.7). In other words, at a certain point the wave period determines the wavelength, or vice versa.

For a given wave period, the greater the water depth, the longer the wave. As waves approach the coast, the wave period may be assumed to remain constant;[4] therefore, as the water depth reduces, so does the wavelength, as determined by equation (2.7). Eventually, the water depth becomes too small for the wave to be viable, at which point it breaks.

4 *Stricto sensu* this holds only if a steady state can be assumed – which is often the case.

Phase celerity (from *celeritas*, Latin for speed or velocity) is the speed at which the wave form (i.e., the wave crest, trough, etc., *but not the wave energy*) travels,

$$c = \frac{L}{T}. \tag{2.8}$$

Combining equations (2.7) and (2.8) yields

$$c = \frac{gT}{2\pi}\tanh\left(\frac{2\pi h}{L}\right). \tag{2.9}$$

For a given water depth, the greater the wave period, the greater the wave celerity, i.e. the faster the wave. This property, *dispersion*, is of great importance in wave theory.[5]

Wave energy density is the amount of energy per unit surface area averaged over the wave period,

$$E = \frac{1}{8}\rho g H^2, \tag{2.10}$$

where ρ is seawater density (as a first approximation, $\rho \sim 1025\,\mathrm{kg\,m^{-3}}$). In the SI wave energy density is expressed in joules per square metre ($\mathrm{Jm^{-2}}$). The term *density* alludes to the fact that the energy is measured *per unit surface area* (per square metre in the SI) in the reference plane (i.e., the quiescent sea surface). It can be proven [35] that the wave energy density is composed of kinetic and potential energy, with equal shares: 50% of kinetic and 50% of potential energy. Importantly, the wave energy density varies with the square of the wave height, so a 2 m wave has four times as much energy density as a 1 m wave.

Group celerity is the speed at which wave energy propagates,

$$c_g = nc, \tag{2.11}$$

with

$$n = \frac{1}{2}\left(1 + \frac{2kh}{\sinh(2kh)}\right). \tag{2.12}$$

Wave power, also known as wave energy flux, is the amount of energy that passes per unit time through a vertical section of unit width perpendicular to the direction of propagation (i.e., parallel to the wave fronts); it is given by

$$P = Ec_g. \tag{2.13}$$

In the SI wave power has units of watts or kilowatts per metre *of wave front* ($\mathrm{Wm^{-1}}$ or $\mathrm{kWm^{-1}}$).

5 In particular in the evolution from a *wind sea* to a *swell*. A *wind sea* occurs when waves are being generated by the wind. In a wind sea, waves of different periods and directions coexist (the wave spectrum is broad-banded). By contrast, in a *swell*, waves have similar periods and directions (the wave spectrum is narrow-banded). (These concepts can be quantified through spectral theory as explained below.) As waves travel away from the area of active wave generation by wind, they do so at different celerities, according to their periods. For this reason, and others of a nonlinear nature, a wind sea transforms gradually into a swell as waves propagate away from their generation area.

So far we have covered linear wave theory. As mentioned above, this theory applies only to certain wave conditions. Other wave theories (Stokes, solitary wave, cnoidal, etc.) are beyond the scope of this chapter, and the interested reader may consult, for example, [36,37].

The wave power over a certain width, b, of wave front may be obtained from

$$P_b = Ec_g b. \tag{2.14}$$

This quantity is useful in establishing the amount of wave power that is available to a WEC, and is the basis of the concept of *capture width*.

2.2.2 Random Waves

In the linear, or Airy, wave theory described in the previous subsection, a wave consists of a sinusoidal oscillation of the free surface. It suffices to observe the surface of the ocean for a couple of minutes or to look at the records of a wave buoy or other wave measuring device to realise that, in fact, the sea surface oscillates following not a sinusoidal curve (a regular wave) but a much more complex pattern (random or irregular waves).

The analysis of random waves is based on the concept of sea state, which may be analysed in the time or the frequency domain. In the time domain we consider a time series of surface elevations, $\eta(t)$, corresponding to a point in space (e.g. the observations from a wave buoy), with a typical duration of between 15 min and 30 min. For the statistical analysis, the hypothesis is made that the surface elevation is a stationary process; for this reason, the time series cannot be too long. Nor can it be too short, or the statistics derived from it (e.g., the significant wave height) would not represent the variability in the sea state properly.

Mathematically the sea state may be described as a Fourier series [38], i.e. a sum of an infinite (in practice, a large) number of harmonic components,

$$\eta(x,t) = \sum_{i=1}^{\infty} a_i \cos(k_i x - \omega_i t), \tag{2.15}$$

with a_i, k_i and ω_i the amplitude, wavenumber and angular frequency, respectively, of the ith harmonic component (or harmonic for short). Each harmonic is, in its own right, a linear regular wave of the type described in the previous subsection. This description of the sea state by means of a Fourier series is based on the principle of linear superposition, a mathematical tool of great potency that forms the basis of the random phase–amplitude model, itself the basis of our wave analysis [39].

The amount of energy available can be quantified in terms of the average wave power or the total energy (total resource) over a certain period of time, e.g. a (typical) year or a (typical) winter. The calculation of the total resource over a certain period based on a time series of wave data is straightforward. Typically, the time series stems from a wave buoy or numerical model and has a three-hourly frequency. In some cases the data consist of a discretised form of the spectral variance or energy density curve, i.e. the values of the spectral curve at a series of frequencies, which give the distribution of the energy in the wave field across frequencies and, if the buoy is directional rather than scalar, also across directions; in other cases, only the characteristic values of the wave parameters are given, e.g. the significant wave height and the energy period.

If spectral density values are given, calculating the characteristic wave parameters is straightforward. Assuming that wave heights are Rayleigh distributed, the significant wave height can be computed from

$$H_s = 4.004\sqrt{m_0} \approx 4\sqrt{m_0}, \tag{2.16}$$

where m_0 is the zeroth-order moment of the variance spectrum,

$$m_0 = \int_0^\infty S(f)\,df, \tag{2.17}$$

with $S(f)$ the spectral variance density. The significant wave height thus obtained can be denoted by H_s or H_{m_0}, the latter notation emphasising the fact that it was calculated from the zeroth-order spectral moment rather than from a time series.

Although the significant wave height is the parameter used most commonly to give the vertical scale of the waves, in certain energy-related applications it may be preferable to use the root-mean-square wave height, H_{rms}, which has a direct interpretation as the wave height of a sinusoidal (Airy) wave with the same energy density as the sea state. Assuming wave heights are Rayleigh distributed [39], the relationship between the significant and root-mean-square wave heights is

$$H_s = \sqrt{2}H_{\mathrm{rms}}. \tag{2.18}$$

The energy period, T_e or T_{m-10}, also has a direct interpretation as the period of the sinusoidal (Airy) wave with the same wave energy flux or power as the sea state in question; it may be obtained from

$$T_e = \frac{m_{-1}}{m_0}. \tag{2.19}$$

Alternatively, the energy period, T_e, may be obtained from the peak period, T_p, assuming a certain theoretical spectral shape. For instance, if a JONSWAP spectrum is assumed, then $T_e = T_p/1.11$. Having defined the significant wave height and the energy period, the wave power, or wave energy flux, of a deep-water sea state may be expressed as

$$P = \frac{\rho g^2}{64\pi} H_s^2 T_e. \tag{2.20}$$

P is the wave power per unit width of wave front, with SI units of watts or kilowatts per metre ($\mathrm{Wm^{-1}}$ or $\mathrm{kWm^{-1}}$). The accuracy of this expression depends on wave heights being Rayleigh distributed. It is therefore valid for most applications in deep water. Using SI units and assuming a typical value of $\rho = 1025\,\mathrm{kg\,m^{-3}}$ for seawater density, the above expression may be approximated as

$$P \approx 0.4906 H_s^2 T_e \approx \frac{1}{2} H_s^2 T_e. \tag{2.21}$$

In this expression, if H_s and T_e are input in m and s, respectively, P is obtained in $\mathrm{kWm^{-1}}$. The above expressions allow the wave power in a sea state to be calculated based on two of its characteristic values, the significant wave height and energy period.

Once wave power is known, the *wave energy* or *wave resource* over a certain period of time, from $t = t_1$ to $t = t_2$, can be obtained by integration with respect to time:

$$E = \int_{t_1}^{t_2} P(t)\,dt, \tag{2.22}$$

where $P(t)$ is wave power as a function of time. As in the case of P, E refers to a unit length of wave front, i.e. it is the wave energy or wave resource *per unit length of wave front* between $t = t_1$ and $t = t_2$, and may be expressed in joules per metre (J m^{-1}) or kilowatt-hours per metre (kWh m^{-1}). The annual resource, i.e. the total energy available from the waves over an entire year, can be calculated by setting t_1 and t_2 to correspond with the beginning and end, respectively, of the year in question.

The mean wave power over a certain period of time, between $t = t_1$ and $t = t_2$, is given by

$$P_{\text{mean}} = \frac{1}{t_2 - t_1} \int_{t_1}^{t_2} P(t)\,dt. \tag{2.23}$$

Usually the analysis is performed on the basis of a time series of characteristic wave parameters (e.g. H_s, T_e) or spectral density curves from which the wave parameters can be obtained. This time series consists of discrete datapoints with a certain frequency, e.g. every 3 hours, and therefore the integrals in the preceding equations must be replaced by discrete summations; for instance, in the case of the mean power, equation (2.23) is replaced by

$$P_{\text{mean}} = \frac{1}{N} \sum_{i=1}^{N} P_i, \tag{2.24}$$

where P_i is the wave power at time

$$t_i = (i-1)\Delta t, \quad \text{for} \quad i = 1, 2, 3, \ldots, N, \tag{2.25}$$

and Δt is the time interval between consecutive data points. If the database has a three-hourly frequency, for instance, then $\Delta t = 10{,}800$ s. By using equation (2.24) the assumption is made that the power value P_i calculated for each data point (each sea state) applies to that time interval, 3 hours in the example, even though the sea state itself is considerably shorter for the reasons outlined above.

2.2.3 Offshore Wave Resource

As mentioned, the quantification provided by overall parameters such as the total annual resource and the mean wave power does not convey sufficient information for the purposes of harnessing the wave resource by means of WECs. It is necessary to *characterise* the resource, i.e. to describe it in terms of the characteristics of the sea states that provide the energy. The most usual characteristic values are the significant wave height (H_s), energy period (T_e) and mean direction (θ_m). If the WECs to be installed are not sensitive to the direction of the waves (e.g. heaving point absorbers) then the situation is simpler, and the main parameters to be considered are the significant wave height and energy period.[6] This information can be obtained based on offshore wave buoy data or, absent these, hindcast data, i.e. time series of wave parameters covering a number of years in the past, generated by a numerical wave model through reanalysis of meteorological data and global, or at least large-scale, atmospheric models [1].

To illustrate the procedure for characterising the wave resource, we present a case study off the Death Coast (*Costa da Morte*, in the vernacular) in Galicia, NW Spain, so called after the large number of wrecks caused by its most energetic wave climate (Figure 2.1). Additional details on the resource in this area may be found in previous work [13,33]. The analysis here is based on data from the directional wave buoy located at 43.49°N and 9.21°W, in 388 m of water depth. Operated by Spain's State Ports, this deep-water wave buoy transmits data at an hourly frequency. The period analysed extends from 15/05/1998 to 26/01/2016. For each data point, the following parameters are available, *inter alia*: significant wave height, energy period, and mean wave direction.

It is convenient to analyse the bivariate distribution of energy period and significant wave height (T_e, H_s) through a *resource characterisation matrix* (the numerical information in Figure 2.2). Each greyed square in the matrix corresponds to a bivariate interval of T_e and H_s, e.g. $T_e = (9.5,10.5)$ s and $H_s = (1.75,2.25)$ m. These bivariate intervals, with lengths of 1.0 s (ΔT_e) and 0.50 m (ΔH_s) in the example, will be referred to henceforth as *energy bins* [13]. The number in each greyed square in the matrix gives the occurrence of the corresponding energy bin or, to be more precise, of the sea states whose values of T_e and H_s fall within the corresponding bivariate interval in the period considered, which may be a particular year, season (e.g. winter 2015), month (e.g. January 2016), or a typical year (defined e.g. as the average of a number of years) or season. In Figure 2.2, the period considered is a typical year in the series from 15/05/1998 to 26/01/2016, obtained by averaging and trimming the data series as appropriate. The occurrence can be expressed in units of time, as in Figure 2.2 (hours), or as a percentage of the total time in the period considered.

The resource characterisation matrix may be regarded as a scatter plot onto which the grid defining the energy bins; is superimposed. Assuming that each data point represents, as in the case study, one hour of real time, the number in each bin in Figure 2.2 is the number of data points in that bin in the scatter plot. Thus, the figure in each energy bin is the occurrence in number of hours in an average year of sea states with values of T_e and H_s that fall into the respective interval.

The curves in Figure 2.2 are wave power isolines, i.e. lines of constant wave power, from 2 kW m^{-1} to 1000 kW m^{-1}, computed based on the deep-water approximation, equation (2.20). The highest values of wave power occur in the upper right-hand corner of the matrix, corresponding to high values of the energy period and, most importantly, the significant wave height. The dependence of wave power on energy period and significant wave height is linear and quadratic, respectively (equation (2.20)).

The resource characterisation matrix may be complemented to form a resource characterisation diagram with information on the contribution of the energy bins to the total resource, which is calculated by adding the energy (wave power times duration) provided by every sea state in the energy bin. This is represented by the grey scale in Figure 2.2. The darker hues, for instance, indicate energy bins providing between 10 and

---

6 Even in the case of heaving buoys some degree of sensitivity to wave directions will always exist due to the layout of the wave farm and the shadow effect of each WEC on the other WECs in its lee.

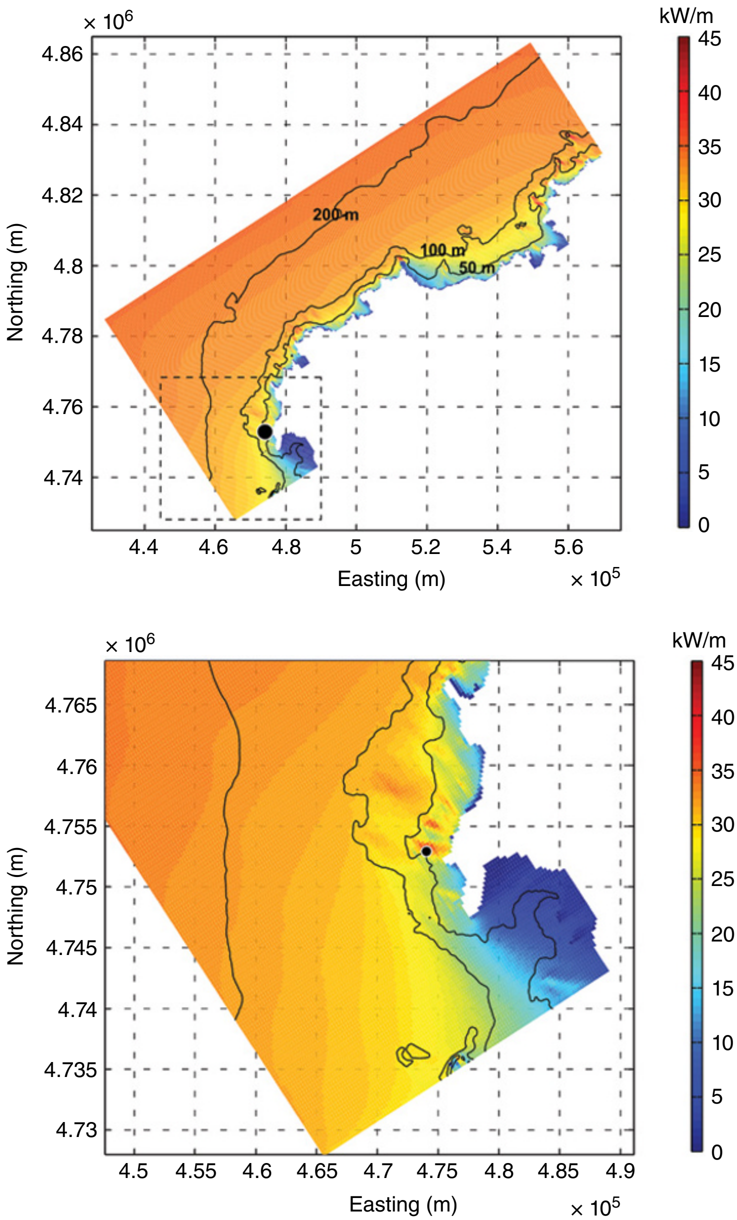

Figure 2.1 The so-called Death Coast (*Costa da Morte*) in Galicia, NW Spain: general map (above) and detailed map of the area around the nearshore hotspot (below), with average wave power values. The nearshore hotspot considered in Section 2.4 is depicted by a black circle.

12 MWh m^{-1} in a typical year. Conversely, the light grey energy bins contribute less than 2 MWh m^{-1}. The advantage of the grey scale is that it makes it easy to visualise immediately which ranges of period and height provide the bulk of the resource in a typical year – and it is on this basis that the WECs to be installed should be selected or designed. This is the *resource characterisation diagram* in Figure 2.2, which consists of

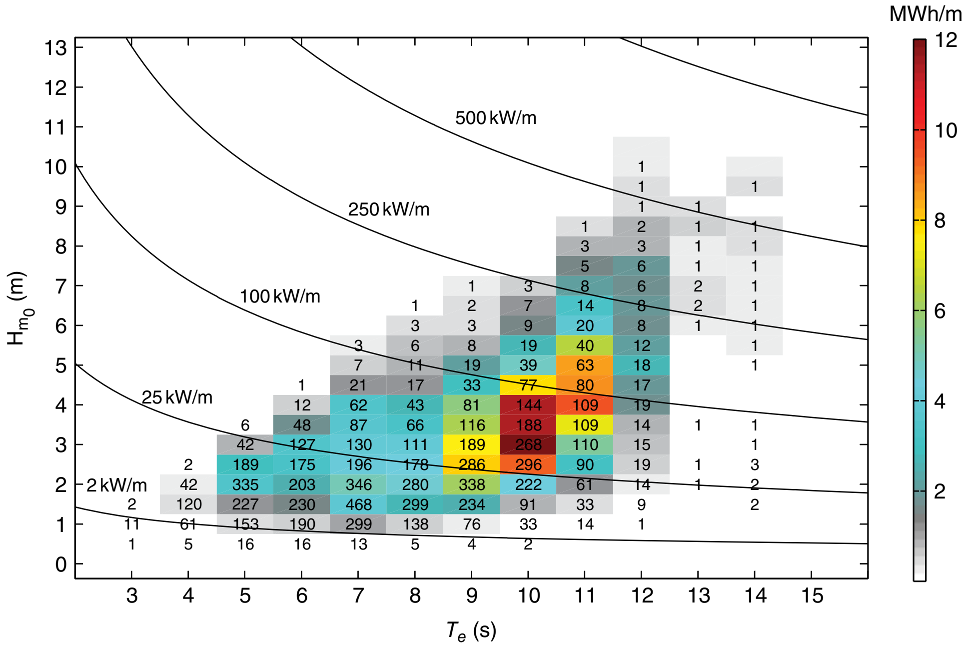

Figure 2.2 Offshore resource characterisation matrix including wave power isolines for the Death Coast (*Costa da Morte*), Galicia, NW Spain. The numbers in the greyed squares represent the occurrence of the respective *energy bins*, expressed in hours in a typical year. The greyscale indicates the contribution of each *energy bin* to the annual resource.

the resource characterisation matrix (the occurrence of the different energy bins), the grey scale (the contribution of each energy bin to the total resource of the period considered) and the wave power isolines.

The contribution of the different energy bins is governed by two factors: the occurrence and wave power of the sea states whose values of T_e and H_s fall within the corresponding interval. The energy bins in the upper right-hand corner of the matrix have high power but low occurrence, therefore contribute little to the overall resource. This does not mean, however, that their most energetic sea states are irrelevant – they need to be taken into account not least with respect to the survivability of the WECs. At the other extreme, the energy bins in the lower left-hand corner of the graph, occurrence values are far higher but wave power is low; therefore, the contribution of these sea states to the total resource is also rather limited. The energy bins that contribute most to the resource (the darkest hues in the central area of the matrix) represent a compromise between occurrence and wave power. In the case study, the bulk of the resource is provided by sea states with significant wave heights between 2.25 m and 5.25 m, and energy periods between 8.5 s and 11.5 s. These high periods are indicative of the oceanic provenance of the waves – to be expected in an area exposed to the long Atlantic fetch. Finally, the energy bins grey with some contribution to the total resource form a triangle with its apex tilted towards the right-hand side (towards the larger periods), which reflects the well-known correlation between wave heights and periods.

For the purposes of calculating the power output from a particular WEC, it is recommended that the resource characterisation matrix for the deployment site be obtained

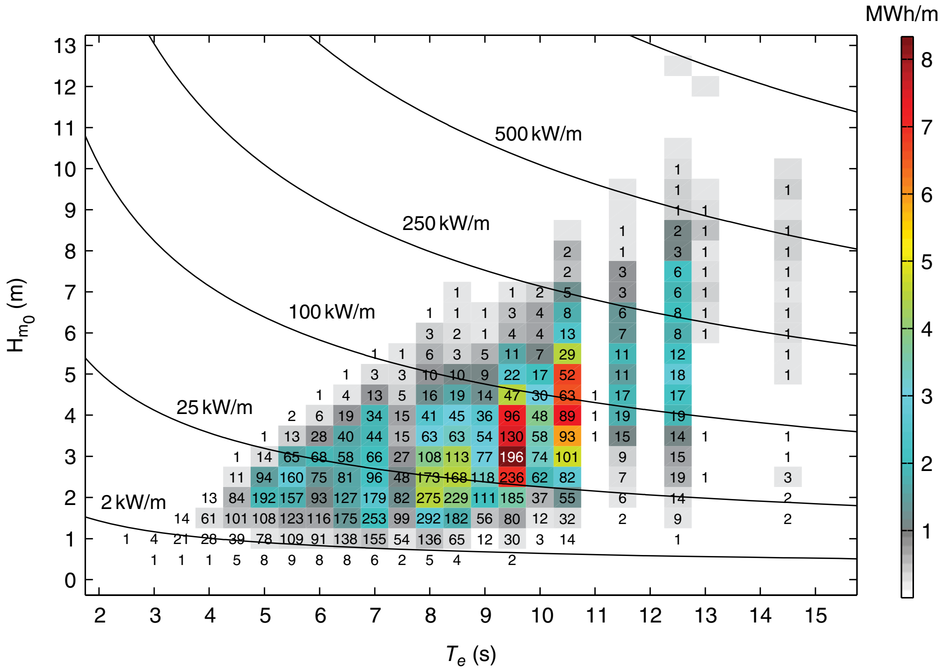

Figure 2.3 Offshore resource characterisation matrix for the Death Coast (NW Spain), with improved resolution: 0.5 s (ΔT_e) × 0.5 m (ΔH_s).

with (at least) the same resolution as the power matrix of the WEC. To expedite the calculation procedure, the offshore resource characterisation matrix should also have the same resolution. In other words, the lengths of the energy bins (ΔT_e, ΔH_s) should match those in the power matrix of the WEC, as should their boundaries. This is of course merely a matter of selecting the energy bins appropriately. For instance, if the resolution of the resource characterisation matrix in Figure 2.2, 1.0 s (ΔT_e) × 0.50 m (ΔH_s), were not enough for a particular WEC, it would be straightforward to produce a refined matrix, e.g. with a resolution of 0.5 s (ΔT_e) × 0.5 m (ΔH_s), as in Figure 2.3.

2.2.4 Nearshore Wave Resource

Having established the offshore wave resource, the next step in characterising the inshore wave resource is the propagation from offshore to the nearshore area of interest. In deep water, by definition, waves do not interact with the seabed. As waves travel towards the coast, water depth decreases; eventually waves reach a water depth at which they begin to 'feel' the seabed. As indicated in Section 2.1, in linear wave theory this water depth is conventionally assumed to be equal to half the wavelength – the depth of the so-called *wave base*. When the wave base 'touches' the seabed, the wave passes from deep water to intermediate or transitional water; in this new regime, it is constrained vertically by the seabed as it continues to propagate towards the shore. This interaction of the wave with the seabed gives rise to a number of physical phenomena, notably refraction and shoaling [35], which affect the wave properties, including the length, celerity, height and power. Importantly, the wave period remains unchanged.

As a result of these processes, the relative spatial uniformity of the resource offshore is transformed into spatial variability nearshore, especially where the bathymetry is highly irregular. In this case, the wave resource is concentrated in particular areas known as n [30], which alternate with areas of comparatively little wave energy. Often drastic changes in the resource occur over distances of the order of hundreds of metres, hence the importance of a fine characterisation of the spatial variability of the nearshore resource. In addition to wave interaction with the seabed, other processes may contribute to the differences between the nearshore and offshore resources, including wave diffraction at headlands or coastal structures, nonlinear wave-wave interactions, energy input from the wind (wave generation) and energy dissipation through whitecapping.

For the purposes of this chapter we assume that the term 'nearshore' signifies an area close to the shore but not so close that waves break because of limited water depth. In other words, we explicitly exclude the surf zone, in which the breaking process dissipates a substantial amount of energy – more or less gradually depending on the type of breaker; for this reason, the resource in the surf zone is typically smaller than elsewhere. In any case, the surf zone, with its highly complex hydrodynamics and high levels of turbulence, would appear to be too harsh an environment to deploy WECs.

Leaving aside bays sheltered by headlands or areas in the lee of structures, there are essentially two reasons why the nearshore wave resource differs from its offshore counterpart: wave interaction with the seabed (refraction, shoaling, etc.) and energy transfer from the wind as waves propagate towards the coast. Assessing the inshore wave resource requires, therefore, that the offshore resource be 'propagated'. This is typically undertaken by means of spectral coastal wave models such as SWAN (Simulating WAves Nearshore), based on the wave action equation [40]. (Wave action density has the advantage over wave energy density that it is conserved in the presence of a current field [41]).

The spectral wave model is implemented onto a computational grid covering the inshore area of interest and extending offshore well into deep water. The geometry of the grid should be adapted to the coastline shape. Cartesian or curvilinear grids may be used; although Cartesian grids are far more common, curvilinear grids have been used advantageously where the coastline is curved [13]. The area of interest should be distant from the grid boundaries – not only from the offshore (ocean) boundary, but also from the lateral boundaries – to prevent numerical disturbances arising at the boundary from affecting the model results in that area.

For the sake of computational efficiency, the resolution of the grid is often not uniform – the grid spacing is smaller in the area of interest, inshore, where wavelengths are usually smaller, than in the deeper sections of the grid offshore. Alternatively, or complementarily, nested grids may be used to reduce the computational cost of the model.

In the case study, the computational grid used for wave propagation off the Death Coast (Figure 2.4) is a Cartesian grid with its x-axis parallel to the general coastline orientation and $\Delta x = 249.9$ m. The y-axis has a variable resolution, from $\Delta y = 888.9$ m at the offshore boundary to $\Delta y = 284.8$ m inshore. The number of nodes along the x and y directions is $m = 577$ and $n = 193$, respectively, with the total number of nodes equal to 111,361.

It is important for the bathymetry to have sufficient resolution, especially in areas where the seabed contours are highly irregular. Bathymetric data are generally available from hydrographic (nautical) charts, and in some cases *ad hoc* surveys of the area of interest may be undertaken. Once this information has been gathered, the water depths at the nodes of the computational grid can be obtained by interpolation.

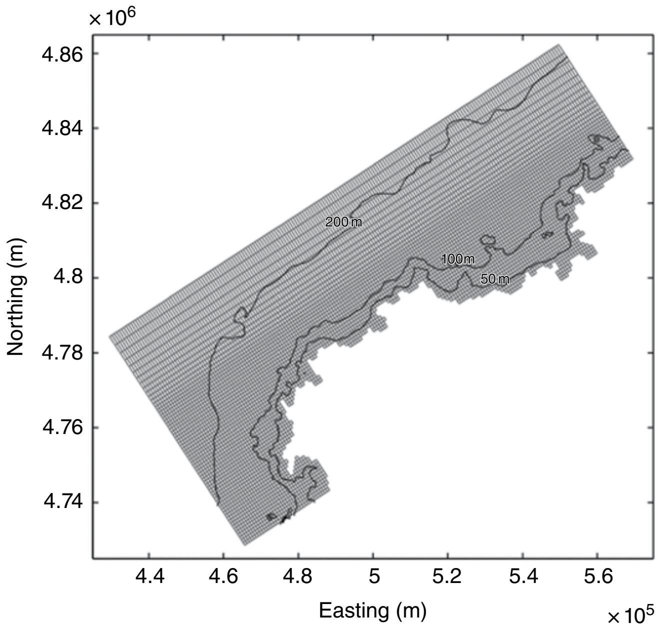

Figure 2.4 Computational grid for the Death Coast case study. For the sake of clarity, only one in three nodes is represented.

Having implemented the numerical model, a number of *wave cases* are then propagated. The number of wave cases should be sufficient to cover the complexity (temporal variability) of the offshore wave resource; in other words, the wave cases should encompass the combinations of wave height, period, direction, etc. that are relevant in the area, so that a substantial proportion of the total wave resource and of the total time in the period considered is covered. In each case the offshore boundary conditions are prescribed based on a certain set of wave parameters (significant wave height, peak period, mean direction, directional spreading, etc.) and spectral shape (e.g. JONSWAP). The straightforward approach is to consider the offshore trivariate distribution of wave height, energy period and mean wave direction, which may be visualised as a 3D resource characterisation matrix similar to that in Figure 2.3, but with an added axis or dimension for the mean wave direction. This is used to select for the propagation one *wave case* for each energy bin, starting with the energy bin with the greatest contribution to the resource and continuing in order of decreasing contribution, until a predetermined percentage of the total resource is covered.

For instance, in the case study, with energy bins of 0.5 s $(\Delta T_e) \times 0.5$ m $(\Delta H_s) \times 22.5°$ $(\Delta\theta)$, a total of 787 wave cases were selected for propagation, representing 95% of the total resource and 88.7% of the total time in the period considered. It may be seen that the offshore resource characterisation matrix that may be constructed based on these wave cases (Figure 2.5) is not dissimilar to the (total) offshore resource matrix (Figure 2.3), which can serve as a basic quality assurance that the number of cases propagated cover large enough proportions of the total resource and of the total time. It would obviously be possible to propagate even more cases and thus cover an even greater percentage of the total resource; however, the important point here is that a compromise between computational cost and accuracy must be struck.

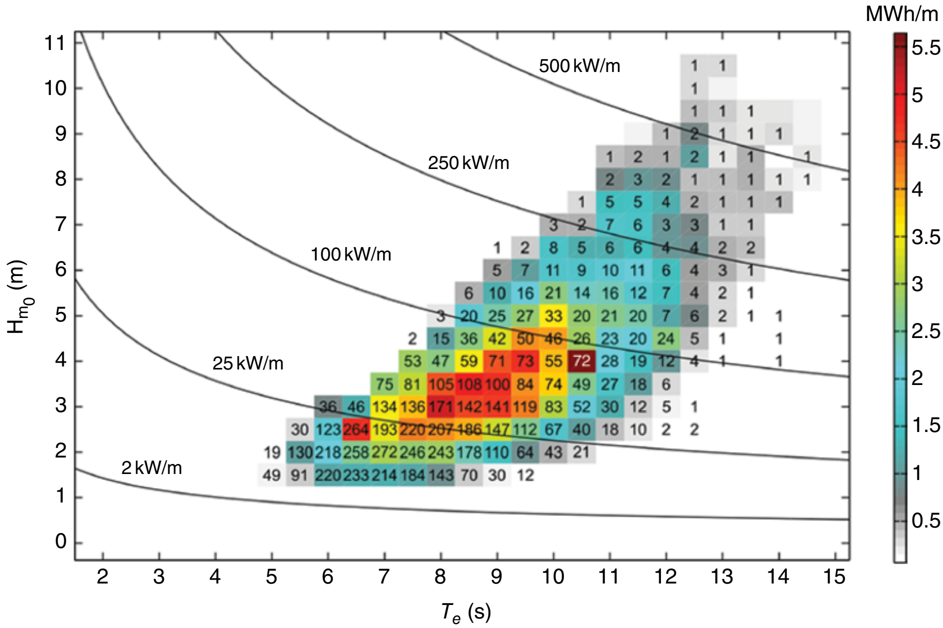

Figure 2.5 Offshore resource characterisation matrix limited to the wave cases selected for propagation, i.e. 95% of the total resource.

The parameters of each wave case for the propagation are then determined so as to represent the sea states in the corresponding energy bin. For the energy period and mean direction, the mid-interval values are usually selected. The significant wave height, however, is another matter: given that the relationship between significant wave height and wave power is quadratic (equation (2.20)), it is recommended that the value selected to represent the interval (H_{s1}, H_{s2}) be $H_{s1} + a(H_{s2} - H_{s1})$, with $a = 2^{-1/2} = 0.7071$.

A numerical model, SWAN [40] in the case study, is now used to propagate the wave cases thus defined. The resource characterisation matrix corresponding to any node of the computational grid is then constructed by adding the contribution of the different cases weighted by their occurrence in the period of time considered (in the case study, a typical year). If the point of interest nearshore does not coincide with a grid node, the results may be interpolated from the values at the surrounding nodes. The calculations are best done by means of a database combined with a decision-aid tool for site selection [33, 42]. In a previous characterisation of the wave resource off the Death Coast [13], the nearshore hotspot in Figure 2.1 was identified. The resource characterisation matrix for this hotspot is presented in Figure 2.6. Here yields a characterisation of nearshore terms.

We have seen that the resource characterisation matrix is a convenient means of representing the bivariate distribution of (T_e, H_s), the main characteristic parameters of the wave resource, whether offshore or nearshore (Figures 2.3 and 2.6, respectively). However, there are cases in which the bivariate distribution (T_e, H_s) is not sufficient, e.g. in designing a wave farm, and must be complemented with the trivariate distribution (T_e, H_s, θ_m), where θ_m is the mean wave direction. The corresponding resource characterisation matrix is now three-dimensional, and therefore not so easy to interpret visually; in fact, 2D representations taking the parameters in pairs may be preferable. For

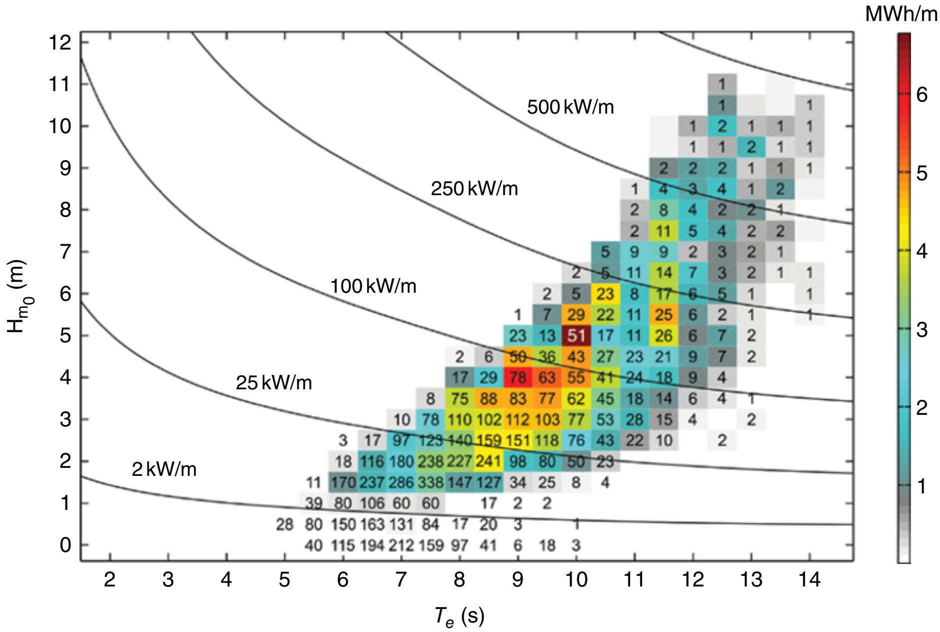

Figure 2.6 Resource characterisation matrix at the nearshore hotspot in Figure 2.1.

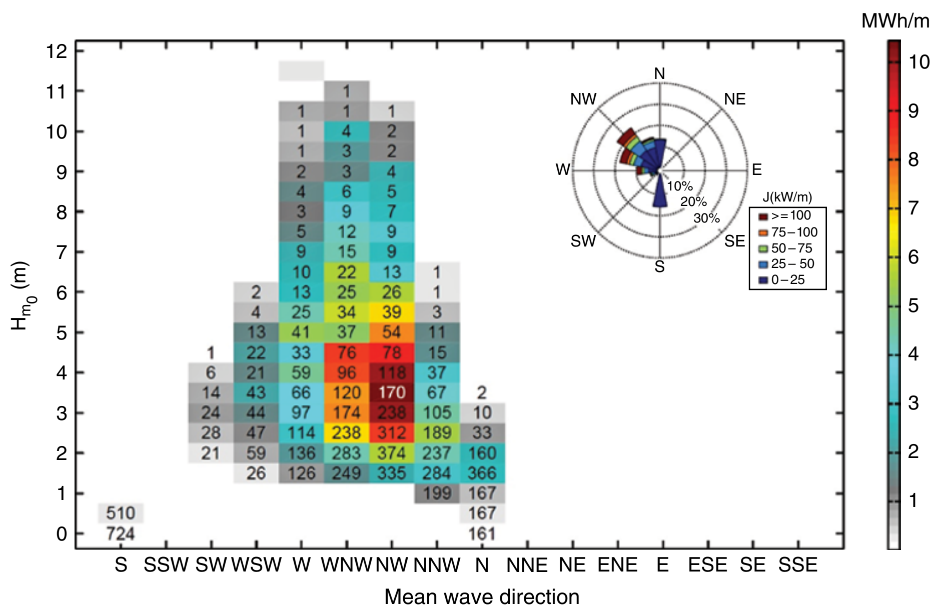

Figure 2.7 Resource characterisation matrix at the nearshore hotspot in terms of mean wave direction and significant wave height (θ_m, H_s). A wave power rose is also included.

illustration, the resource characterisation matrices for the nearshore hotspot in terms of (θ_m, H_s) and (θ_m, T_e) are presented in Figures 2.7 and 2.8, respectively, complemented with a wave power rose. It is apparent that the lion's share of the resource is provided by waves from the IV quadrant, primarily from the northwest.

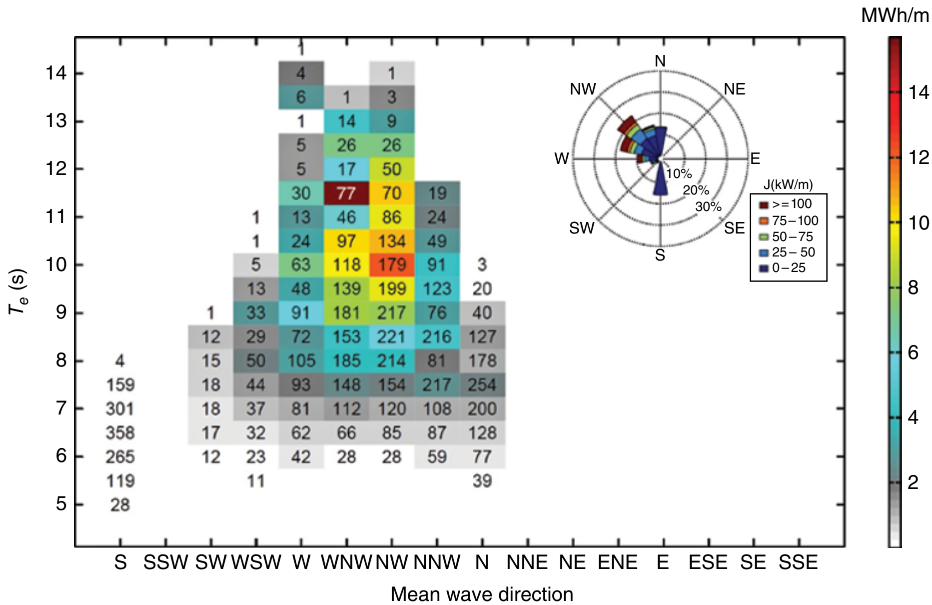

Figure 2.8 Resource characterisation matrix at the nearshore hotspot in terms of mean wave direction and energy period (θ_m, T_e). A wave power rose is also included.

2.3 The Tidal Stream Resource

2.3.1 Fundamentals of the Tide

The tide is the periodic oscillation of the sea level caused by the gravitational attraction of the Moon and Sun acting on the water particles in the hydrosphere. The force driving the tide is controlled by the complex motion of the Earth–Moon–Sun system. In spite of the much larger mass of the Sun, solar attraction plays a lesser role, approximately 46% of lunar attraction, due to the greater distance from the Earth to the Sun than to the Moon. Tides are different across the globe, with many coastal regions experiencing only very weak tides (e.g. enclosed seas such as the Mediterranean) while others are subjected to large tidal oscillations. This is due to the fact that the oscillation driven by this astronomical forcing propagates as a long wave in an ocean or sea with particular characteristics (water depths, boundaries) and under the effects of the Coriolis force. Indeed, this long wave is refracted over the continental shelf, reflected at land boundaries, amplified by the tapering banks of estuaries or by resonance, dampened by friction with the seabed, etc. In sum, the tide is a complex phenomenon driven by astronomical forces but controlled locally by the bathymetry and coastline geometry of the estuary, gulf, or sea concerned, and of the ocean basin to which it is connected.

Tides have been known since Antiquity, but their explanation has eluded scientists for many centuries, including eminent names such as Galileo. It was not until Newton and his theory of gravity that the primary cause of the tide was understood. However, the differences in the tide between regions could not be explained until much later, when Laplace introduced the concept of the tide as a wave propagating over a sea with certain water depths and boundaries (coastlines). A complete description of the theory of tides is beyond the scope of this book, and the interested reader may consult [43].

As a periodic oscillation, the tide is described as a long wave that propagates over oceans, seas and estuaries, with the usual properties of waves, e.g. wave length and amplitude. When the crest or trough of the wave reaches a particular point, this point is at high or low water, respectively. The period of the tide, or time interval between two consecutive high waters, is approx. 12 h 25 min in the case of semidiurnal tides (usual in the Atlantic Ocean and other regions), and 24 h 50 min in the case of diurnal tides (in some areas of the Pacific Ocean, Gulf of Mexico, etc.) The terms semidiurnal and diurnal allude to the duration of one tide, approximately a half day or one day, respectively.

The difference in elevation between consecutive high and low water is called the tidal range, which varies in space and time, i.e. at any given point two tides will have different tidal ranges. The tidal range in the open ocean is never really large; it can, however, become large near shore, particularly in semi-enclosed seas and estuaries, due to resonance and convergence of the land boundaries [43]. A conspicuous case is the Bay of Fundy, Canada, where the tidal range reaches 16.3 m. Coastlines are classified as microtidal, mesotidal or macrotidal when the tidal range is below 0.5 m, between 0.5 m and 4.0 m, and above 4.0 m, respectively.

Semidiurnal tides vary with a fortnightly period (14.8 days, or half the lunar month). At new or full moon, when the Moon, Sun and Earth are aligned (in syzygy), the solar tide reinforces the lunar tide, which results in particularly large tidal ranges (spring tides) shortly afterwards. The reason for the lag between the syzygy (the full or new moon) and the maximum tidal range is the inertia of the water mass. Half a lunar month, i.e. 14.8 days, later, at the first or last quarters, the Moon and Sun are orientated at a 90° angle relative to the Earth (in quadrature) and the opposite occurs: the solar effects reduce the lunar tide, which leads to particularly small tidal ranges (neap tides).

Another relevant aspect of the astronomical forcing of the tide is the varying distance between the Moon and the Earth, leading to increased and decreased tidal ranges at the lunar perigee and apogee – when the Moon is closest and farthest from the Earth in its orbit, respectively. The period of this oscillation is 27.55 (solar) days. The largest tides occur, therefore, when spring tides coincide with the lunar perigee.

The periodic oscillation of the sea level at a given point may be described mathematically by means of a Fourier series

$$\zeta(t) = \sum_i a_i \cos(\omega_i t + \phi_i), \tag{2.26}$$

where t is time, $\zeta(t)$ is the tidal level, and a_i, ω_i and ϕ_i are the amplitude, angular frequency and phase of the ith harmonic component, respectively. The summation is performed over a large number of harmonic components or *tidal constituents* – the larger the number, the greater the accuracy. Seven or eight may suffice in most cases, although in certain areas more may be required, for instance in estuaries with tidal asymmetry.[7]

The angular frequency of a given tidal constituent is the same at any point on the planet: it is determined by the relative motions of the Earth–Moon–Sun system. However, the amplitudes and phases of the constituents vary from point to point, as does the tidal range. The main tidal constituents at the mouth of the Severn Estuary are shown in Table 2.1.

The semidiurnal or diurnal character of the tide depends on the relative amplification of certain tidal constituents, which is measured by the tidal form factor, also known as the F-factor [45],

$$F = \frac{K_1 + O_1}{M_2 + S_2}, \tag{2.27}$$

where K_1, O_1, M_2 and S_2 represent the amplitudes of the corresponding tidal constituents (Table 2.1). It may be seen that the constituents in the numerator and denominator are, respectively, the principal diurnal and semidiurnal constituents. It follows that high and low values of F will correspond to diurnal and semidiurnal tides. To be more precise, for $F < 0.25$ or $F > 3$, the tidal regime is semidiurnal or diurnal, respectively. For the intermediate values an intermediate regime exists, predominantly semidiurnal or diurnal for $0.25 < F < 1.5$ or $1.5 < F < 3$, respectively.

So far we have discussed the astronomical tide, but this is not the only cause of variations in sea level. The meteorological tide is the change in sea level due to winds and changes in atmospheric pressure. When the wind blows onshore, shear stress on the sea surface causes the surface level to rise near shore; we could say that water 'piles up' against the coast; conversely, when the wind blows offshore, nearshore surface tidal levels drop. As regards atmospheric pressure, the effects of its variations on surface levels are easy to understand if we consider that the sea surface is, in reality, the interface between two fluids, air and seawater. When atmospheric pressure rises above its standard value at sea

Table 2.1 Tidal constituents at the mouth of the Severn Estuary [44].

Constituent	Description	Amplitude (cm)	Phase (°)
M_2	Principal lunar semidiurnal	235.24	156.87
S_2	Principal solar semidiurnal	84.17	201.21
N_2	Larger lunar elliptic semidiurnal	44.79	138.48
K_2	Lunisolar semidiurnal	24.45	195.80
K_1	Lunar diurnal	6.77	127.34
O_1	Lunar diurnal	6.70	351.17
P_1	Solar diurnal	2.23	121.81
Q_1	Larger lunar elliptic diurnal	1.95	305.66
M_4	Shallow water overtides of principal lunar constituent	3.69	290.99

7 In which case it is important to include the M_4 (overtide) harmonic.

level (1013 HPa) – in an anticyclone or high pressure – surface levels drop; conversely, when the pressure decreases below 1013 HPa – in a depression or low pressure – surface levels rise. With 1 HPa of pressure variation causing 1 cm of tidal level change, the meteorological tide is generally well below ±0.5 m; it can, however, reach much larger values under storm conditions (storm surge). In a hurricane the storm surge can reach several metres, as it did during the infamous Hurricane Katrina (2005) [46].

For a given point, a harmonic analysis can be carried out based on a time series of tidal levels (e.g. from a tide gauge) to determine the amplitudes and phases of the tidal harmonics. A tide gauge records the oscillations of sea level over time, which are caused by the astronomical tide and other factors, notably the meteorological tide, infragravity waves and wind waves. For this reason, the data series should be pre-treated prior to the harmonic analysis so that the influence of the non-astronomical factors is removed. Removing short waves is straightforward by means of a low-pass filter; other techniques (e.g. wavelets) may also be applied [47–49]. Involved the effects of atmospheric pressure changes may be extracted easily if a time series of atmospheric pressure at or near the tide gauge is available, but removing the effects of winds before the harmonic analysis may be more complicated [50–52].

Once the effects of the main non-astronomical factors on the time series of tidal level have been extracted, the harmonic analysis may be performed. Essentially, it is a means of translating information from the time domain into the frequency domain. The fast Fourier transform (FFT) [47,53] is the most popular tools. Based on the time series of tidal level (ζ_i, for $i = 1, 2, 3, \ldots$), the FFT yields the amplitudes and phases of the harmonics or tidal constituents.

For the harmonic analysis to yield accurate values, the time series must be sufficiently long. In theory, 18.6 years (the nodal period of the Moon) would be the minimum time to cover the full complexity of the motions of the Earth–Moon–Sun system. In practice, however, such a long a time series for a particular location may not be available, and 8–10 years may be considered sufficient for many applications. Of course, the difficulty is that at many sites of interest there is no tide gauge, so that no time series of observed tidal levels is available. In this case, the alternative is to use a global database such as TOPEX/Poseidon, which gives the amplitudes and phases of the tidal components at any point, based on a global ocean model and satellite altimetry [54–57]. Having obtained the amplitudes and phases of the main constituents, the truncated Fourier series enables tidal energy developers or coastal engineers to predict tidal level oscillations at a point of interest with considerable accuracy. This predictability is arguably one of the great advantages of tidal energy relative to other renewable energy sources.

2.3.2 Tidal Barrage or Lagoon vs. and Tidal Stream

There are essentially two methods for harnessing the energy of the tide. The first consists of building a tidal barrage or lagoon in an estuary or other semi-enclosed body of water with a significant tidal range. With the barrage sluices closed, a difference in elevation is established between the two sides of the barrage or lagoon as the tidal level rises or falls on the sea (outer) side. Eventually, the sluice gates are open, and the flow through them drives turbine-generator groups. The second method consists of deploying turbines in the free flow of water caused by the tide (the tidal stream) to harness its kinetic energy.

The potential energy of the water mass impounded by a tidal barrage or lagoon has been used since antiquity. Modern-day applications to generate electricity include the tidal power stations at La Rance (France) and Sihwa Lake (South Korea), which have operated since 1966 and 2011, respectively, with rated power of 240 MW and 254 MW. For all their interest, tidal barrages have a number of disadvantages which may hinder prospective developments: the number of potential sites is very limited, their environmental impact is potentially considerable and a large capital investment is required before the first kilowatt-hour is produced. These disadvantages are mitigated in the case of tidal lagoons, and they are currently under consideration for certain areas (S Wales, UK). In any case, many more sites are available for tidal stream farms, their environmental impact is lower, and the financial aspects are less challenging. Consequently, the focus of this chapter is on the tidal stream resource.

2.3.3 The Tidal Stream Resource

The tidal stream resource may be defined as the kinetic energy in tidal currents, i.e. horizontal motions of water caused (primarily) by the tide; other agents may also play a role, e.g. riverine flow, winds, salinity or temperature gradients.

The tidal stream power through a cross-section Ω normal to the flow is the flux of kinetic energy through that section,

$$P_\Omega = \frac{1}{2}\alpha\rho\bar{v}^3 A_\Omega, \tag{2.28}$$

where $\bar{v}$ is the magnitude of the flow velocity (the speed of the current) averaged over Ω, A_Ω is the surface area of section Ω, ρ is the density of water, and α is the energy coefficient [45],

$$\alpha = \frac{1}{\bar{v}^3 A_\Omega}\int_\Omega v^3 \mathrm{d}A, \tag{2.29}$$

with v the magnitude of the flow velocity at a generic point of the section Ω and dA the differential area. P_k has units of watts in the SI.

The tidal stream power given by equation (2.28) is the amount of kinetic energy that crosses the section considered (Ω) per unit time. This is the power *available* in the tidal stream flow; however, not all of this tidal stream power can be transformed into mechanical power (and later on into electrical power) by the turbine-generator group, due to Betz's law and the mechanical and electrical losses in the system.

The energy coefficient, α, takes into account the variations in flow speed over the section considered, Ω. If the speed is uniform within the section, then $\alpha = 1$; this case is, however, only of academic interest. In the general case, i.e. when the magnitude of flow velocity flow speed does vary within the section, α is higher than unity, for the average of the velocity cubed is always higher than the average velocity cubed. The actual value of α will depend on the flow characteristics, the section and point in time considered, with typical values slightly above unity; for instance, if the section is a transect of a wide channel, a value of $\alpha = 1.03$ is recommended [58]. In the absence of better data, a value $\alpha \approx 1$ is often assumed as an approximation, which amounts to neglecting the variation of v within the section considered, and leads to the following conservative estimate of tidal stream power:

$$P_\Omega \approx \frac{1}{2}\rho v^3 A_\Omega. \tag{2.30}$$

Importantly, area A_Ω must be normal to the flow.

On these grounds, *tidal stream power density* may be defined as the tidal stream power passing through a unit surface area normal to the flow,

$$p = \frac{1}{2}\rho v^3, \tag{2.31}$$

where p has SI units of watts per square metre. The tidal stream power available to a turbine may be obtained by multiplying the tidal stream power density by the rotor (swept) area.

If the variation of the flow speed, v, with time is known (typically through numerical modelling), then the power density may be integrated with respect to time to obtain the *tidal stream energy density*:

$$e = \int_{t_1}^{t_2} p(t)\,dt, \tag{2.32}$$

where the interval of integration considered, (t_1,t_2), may be e.g. a spring-neap tidal cycle or a typical one year. The tidal stream energy density may be expressed in joules per square metre or kilowatt-hours per square metre.

If the interval of integration is one year, the *annual tidal stream energy density* is obtained; to reduce the computational cost for of the numerical model, an approximation may be obtained by performing the integration over a tidal (spring-neap) cycle, and extrapolating the result to one year.

In certain cases it may be of interest to consider the *tidal stream power per unit width*, i.e. the flux of kinetic energy through a vertical section normal to the flow of unit width, extending from the seabed to the surface [59]; this is given by

$$P_u = \frac{1}{2}\int_{-h}^{0} \rho(z)\left[v(z)\right]^3 \mathrm{d}z, \tag{2.33}$$

where $v(z)$ and $\rho(z)$ are, respectively, the flow velocity magnitude and water density as a function of z, the vertical coordinate; $z = 0$ at the reference plane (the quiescent water level) and $z = -h$ at the seabed, i.e. the z-axis is positive upwards. P_u has SI units of watts per metre.

The variation of density with depth may be caused by differences in salinity and temperature (especially in stratified estuaries) or by the weight of the water column above the level considered; in nearshore waters, where tidal stream sites are located, water depths are not large, of the order of $O(10^1\,\text{m})$, and the latter effect is negligible. In any case, the variations in $\rho(z)$ nearshore are generally below 3%, and can be disregarded for our purposes here. Under the assumption $\rho(z) \approx \text{const.} = \rho$, equation (2.33) simplifies to

$$P_u = \frac{1}{2}\rho\int_{-h}^{0} \left[v(z)\right]^3 \mathrm{d}z. \tag{2.34}$$

An energy coefficient could be easily defined for the vertical section of unit width along the lines of α in the preceding section [59]. It is also possible to neglect the variation of $v(z)$ altogether, i.e. to replace $v(z)$ by the depth-averaged flow velocity magnitude,

$$\overline{v_u} = \frac{1}{h}\int_{-h}^{0} v(z)\mathrm{d}z, \tag{2.35}$$

which yields

$$P_u \approx \frac{1}{2}\rho h\left(\overline{v_u}\right)^3. \tag{2.36}$$

Similar to the previous case of an arbitrary section Ω, neglecting the variability of the flow velocity magnitude in the vertical section of unit width, i.e. replacing equation (2.34) by equation (2.36) in the calculation of the tidal stream power per unit width, leads to a conservative estimate.

2.3.4 Selection of Potential Tidal Stream Sites

Multiple aspects must be considered in the selection of a site for installing a tidal stream farm, i.e. an array of tidal stream turbines or, more generally, tidal energy converters, including the tidal stream resource, the environmental impact on the area, other uses of the marine space, and the connection to the electricity network. The tidal stream resource available in the area is fundamental among these aspects. In the previous section we have seen that tidal stream power is a function of the velocity of the current cubed.

For tidal currents to be significant, the tidal range must be relevant. For instance, in the Mediterranean Sea, where most coastlines have tidal ranges below 0.5 m, the tidal stream resource is negligible. However, although a significant tidal range is a *conditio sine qua non*, it is not sufficient for strong tidal currents to occur. Indeed, on coasts open to the ocean tidal currents are typically negligible, even if the tidal range is not. Tidal flows only become relevant when a substantial tidal range occurs in a semi-enclosed body of water, such as a sea, bay, estuary, ria or fjord.[8] Examples are the Severn Estuary and the Bristol Channel (UK) [17,44,60–62], the North Sea, in particular in areas such as the Pentland Firth (UK) [63,64] or Orkney (UK) [65], the Bay of Fundy (Canada) [66] or the estuaries (rias) of Ribadeo [67], Ortigueira [68,69], Muros [45] and Arousa [70] in NW Spain. Within these semi-enclosed bodies of water tidal currents tend to be particularly strong at certain transects where the coastline geometry constrains the flow.

At many of these constrictions, water depths are limited, and may preclude in some cases tidal stream energy exploitation. From equation (2.36) it is clear that tidal stream power per unit width depends on the magnitude of the flow cubed and the water depth. For this reason, it makes sense to consider tidal flow and water depth conjointly in assessing the suitability of an area for tidal stream exploitation. This is the rationale behind the Tidal Stream Exploitability (TSE) index [59], which combines information on the tidal flow intensity and water depths with certain technical constraints relating to the exploitation of tidal stream power by means of tidal stream turbines. In certain areas it may be important to consider wave action in assessing the tidal stream energy resource [71]. The role of the type of turbine in the actual power than can be produced

8 Rias and fjords are two particular types of estuary.

at a given site is also important, and significant differences in the power output may exist between floating and fixed (bottom-mounted) turbines [72].

In the equations in the previous subsection the magnitude of the flow velocity is cubed; therefore, a small difference in velocity gives rise to a great difference in power [68]. For instance, an increase of a mere 20% in the speed of the tidal current implies 72.8% more tidal stream power. For this reason, in characterising the tidal stream resource of an area it is crucial to determine the velocity field and its fluctuations with great accuracy. Without numerical modelling, this would require measuring tidal currents at a large number of stations in the area of interest over long periods of time, which would be an expensive, time-consuming procedure. Fortunately, it is possible to reduce the number of stations and the duration of the observations thanks to numerical modelling.

To characterise the tidal stream resource in an area of interest, a numerical model of the hydrodynamics of the area is implemented, calibrated and validated based on field data. Once validated, the model results can be trusted to represent faithfully the actual flow field and its variability. The application of numerical modelling to the characterisation of the tidal resource is the topic of the following subsections.

2.3.5 Implementation of the Numerical Model

The numerical models used to characterise the tidal resource are based on the Navier–Stokes equations:

$$\frac{\partial u}{\partial x}+\frac{\partial v}{\partial y}+\frac{\partial w}{\partial z}=Q, \tag{2.37}$$

$$\left.\begin{aligned}\frac{Du}{Dt}&=fv-g\frac{\partial \zeta}{\partial x}-\frac{g}{\rho_0}\int_{z'=z}^{z'=\varsigma}\frac{\partial \rho}{\partial x}dz'+\upsilon_h\left(\frac{\partial^2 u}{\partial x^2}+\frac{\partial^2 u}{\partial y^2}\right)+\upsilon_v\left(\frac{\partial^2 u}{\partial z^2}\right)\\ \frac{Dv}{Dt}&=-fu-g\frac{\partial \zeta}{\partial y}-\frac{g}{\rho_0}\int_{z'=z}^{z'=\varsigma}\frac{\partial \rho}{\partial y}dz'+\upsilon_h\left(\frac{\partial^2 v}{\partial x^2}+\frac{\partial^2 v}{\partial y^2}\right)+\upsilon_v\left(\frac{\partial^2 v}{\partial z^2}\right)\end{aligned}\right\}, \tag{2.38}$$

$$\frac{\partial p}{\partial z}=-\rho g, \tag{2.39}$$

$$\frac{Dc}{Dt}=D_h\left(\frac{\partial^2 c}{\partial x^2}+\frac{\partial^2 c}{\partial y^2}\right)+D_v\frac{\partial^2 c}{\partial z^2}-\lambda_d c+R_s, \tag{2.40}$$

where the coordinates x, y and z are directed along the east, north and vertical directions, respectively, with u, v and w the components of the flow velocity along the respective directions; ζ is the elevation of the free surface with respect to the reference level; ρ and ρ_0 are the density and reference density of seawater, respectively; Q is the intensity of mass sources per unit area; f is the Coriolis parameter; g is the gravitational acceleration; υ_h and υ_v are the horizontal and vertical eddy viscosity coefficients, respectively; c may stand for salinity or temperature; D_h and D_v are the horizontal and vertical eddy diffusivity coefficients, respectively; λ_d represents the first-order decay process; and R_s is the source term.

Equation (2.37) is the continuity equation, which expresses the conservation of fluid mass. Equations (2.38) express the momentum balance (Newton's second law) in the horizontal directions (x, y). Equation (2.39) expresses the momentum balance in the vertical direction under the Boussinesq approximation. Finally, equation (2.40) is the transport equation, which is solved for both salinity and temperature.

The Boussinesq approximation assumes that even though the density does vary along the vertical, the primary influence of this variation as regards fluid stability is on the body force rather than on the acceleration term, so that the latter may be neglected; in other words, the variation of density may be ignored in the momentum equations except in respect of the gravitational term [73].

Equations (2.37)–(2.40) are in three dimensions; in some cases, where the three-dimensional features of the flow are negligible (e.g. in well-mixed estuaries), these equations may be replaced by a set of equations in the two horizontal dimensions (plus time) by integrating vertically the velocity and other relevant variables from the seabed to the surface [45, 74].

With the exception of certain highly simplified cases, the solution of the Navier–Stokes equations can only be accomplished through a numerical model. To this end, both the equations and the computational domain must be discretised. The details of the discretisation of the governing equations are discussed further in Chapter 8. A number of 'off-the-shelf' software packages exist to solve the above set of equations, e.g. Delft3D or MIKE21, which can operate in either two-dimensional horizontal (2DH) or 3D mode.

As regards the discretisation of the computational domain, the grid is generally Cartesian in the horizontal plane (coordinates x, y), although curvilinear grids can be used if they are better suited to the geometry of the area to be modelled. For the vertical coordinate, the standard Cartesian approach of a z coordinate would lead to different numbers of vertical layers across the domain to accommodate the changing water depth, which might compromise numerical efficiency. For this reason, the so-called σ-coordinate approach is generally preferred [75, 76].

A Dirichlet condition is usually prescribed along the outer (ocean) boundary, in which the variation with time of sea surface elevation is prescribed, alongside salinity and temperature. The elevation itself is calculated based on the tidal harmonics or tidal constituents, which are typically obtained from a global database, itself obtained from large-scale (global) numerical modelling and satellite altimetry (e.g. TOPEX/Poseidon [54, 55, 57]). Alternatively, the Dirichlet boundary condition can be combined with Neumann boundary conditions, in which the rate of change of elevation rather than the elevation itself is prescribed, to form a mixed open boundary condition. This approach has been shown to reduce the generation of numerical disturbances at the boundary [77, 78].

Importantly, the number of tidal harmonics must be sufficient to capture the complexity of the tide in the area. At least seven harmonics must generally be taken into account. In the case of estuaries with significant tidal asymmetry, the relevant harmonics must be included, notably the M4 (overtide) [65, 79]. Salinity and temperature at the ocean boundaries may be prescribed based on measurements or large-scale modelling. At the seabed, bed shear stress is typically accounted for by means of a quadratic stress law, and where relevant, the wind stress at the surface can also be prescribed [76, 80].

For the inner (land–water) boundaries, a null flow, free slip boundary condition is usually adopted [81]. At a river mouth, the flow into the computational domain is taken into account by specifying the time variation of the riverine inflow and its temperature at the boundary.

In the inner sections of estuaries, intertidal areas are common, which flood and dry with the tide. This means that the computational domain and its boundaries change with the tide, and the numerical scheme must be capable of handling this without compromising its stability. Typically grid points are removed when the tide falls and added again when it rises.

Having prescribed the boundary conditions, the initial condition is usually the so-called *cold start*, in which the flow velocity and surface elevation are assumed to be null throughout the computational domain. This is obviously unrealistic, and is only assumed for the sake of simplicity. As a result, in the initial period of the simulation the model variables do not represent the real hydrodynamics in the domain, and care must be taken to exclude the results from this *spin-up* period from the analysis. As a conservative assumption, the spin-up period can be assumed to extend 1 month, after which the model results are assumed to be correct, subject to calibration and validation.

Importantly, the model must be calibrated and validated based on field measurements. Calibration consists of running the model, comparing the results with the observations (of tidal level, flow velocity, salinity, temperature), tweaking certain model parameters (the calibration parameters), then running the model and comparing its results again, and repeating this cycle until the differences between the model results and the observations, which can be quantified by means of e.g. the correlation coefficient or the root-mean-square error (RMSE), are negligible. At this point the model has been validated, and its results can be assumed to represent the actual hydrodynamics and salinity and temperature fields in the computational domain. Typical calibration parameters are the eddy viscosity or the seabed roughness [82, 83].

As regards the hydrodynamics, the field data for calibration and validation should ideally comprise both surface elevation (tidal level) and flow velocity data [69]. These data can be collected by means of acoustic Doppler current profilers (ADCPs) deployed on the seabed, attached to some structure (e.g. a pier or bridge pile) and even mounted on a boat, in which case the boat motion must be accounted for. ADCPs yield profiles of flow velocity, which can be vertical or horizontal depending on the orientation of the device, and pressure at the location of the instrument, which can be converted into tidal level. ADCP data often require de-noising, which can be carried out by means of wavelets (e.g. stationary wavelet transforms [82]), among other methods; an in-depth revision of data analysis methods is provided by [47]. If there are ports with tidal gauges within the domain, these are naturally a useful means to obtain tidal level data. Certain (simplified) current velocity data can also be obtained from hydrographic charts (e.g. *tidal diamonds*). Wherever possible, the calibration and validation of the model should be based on data not only of tidal level but also of flow velocity, ideally from observations at two or more points in the model domain. An alternative approach is to carry out the calibration and validation by comparing the tidal harmonics obtained from a harmonic analysis of tidal gauge data with those calculated based on model results [82]. As in the previous approach, two or more points should be used. As regards the validation of salinity and temperature, vertical profiles can be collected from a boat by means of a CTD sensor – which measures conductivity, temperature and pressure.

2.3.6 Case study I: Bristol Channel and Severn Estuary

In this subsection, the procedure is illustrated through a case study in the Bristol Channel and Severn Estuary, an area of great potential for tidal stream [17, 44, 60–62] (and tidal barrage [84]) development, in which a model based on the 2DH equations is implemented. A summary is presented here; more details can be found in [17]. The study area extends from the mouth of the River Severn to the Celtic Sea, with its ocean boundary between Trevose Head and St. Govan's Head (Figure 2.9).

The computational grid had a resolution of 500 × 500 m. Water depths were interpolated from the GEBCO data set. As regards the boundary conditions, the tidal forcing was prescribed along the ocean boundary based on the main nine constituents, which were obtained for eight nodes of the boundary by means of the TPXO 7.2 global database [85]. Values at intermediate nodes were interpolated. Salinity and temperature

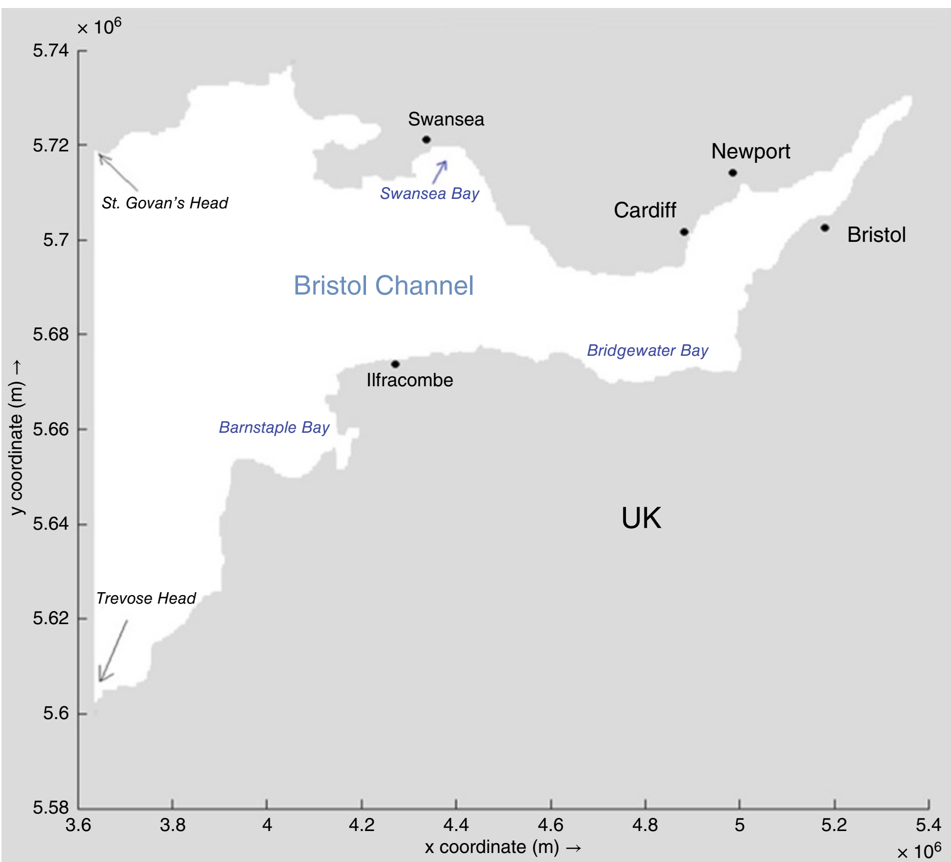

Figure 2.9 The Severn Estuary and Bristol Channel (case study I).

values at the boundary were obtained from the British Oceanographic Data Centre (BODC). At the land boundaries, null flow, free slip conditions were prescribed.

The period of interest considered for the simulation was a complete tidal cycle extending from 14/03/2011 to 28/03/2011. As explained in the preceding subsection, the model simulation covered not only the period of interest but also a spin-up period of 31 days. The initial conditions were null surface elevation and velocity throughout the grid (cold start). The calibration parameter was the horizontal eddy viscosity; on the basis of previous work [17], a value of $30\,\text{m}^2\,\text{s}^{-1}$ was selected.

For validation, the model results were compared with tidal levels from four tidal gauges operated by the UK Tide Gauge Network (BODC) and tidal stream data from five tidal diamonds from Admiralty Chart No. 1165. The comparison of tidal levels (Figure 2.10) shows excellent agreement (with correlation coefficient values $R > 0.97$). As regards velocities, the goodness of fit between model results and field data is quantified in Table 2.2, again with excellent results [17]. Once validated, the model was used to calculate the annual energy density (Figure 2.11). In certain hotspots values are well above 60 MWh m^{-2}, reaching up to 90 MWh m^{-2} [62].

2.3.7 Case Study II: Ria de Ortigueira

The second case study is Ria de Ortigueira, an estuary in Galicia (NW Spain) with a maximum tidal range of 4.5 m (Figure 2.12) [69, 82]. The computational grid (Figure 2.13) is Cartesian, its x- and y-axis orientated west–east and south–north, respectively. The horizontal resolution varies through the domain for the sake of computational efficiency, with a grid spacing of $50 \times 50\,\text{m}$ ($\Delta x \times \Delta y$) within the ria (the area of interest), becoming coarser along the y-axis outside the ria, up to $50 \times 150\,\text{m}$. The bathymetry was interpolated from nautical charts 408 and 4083 of Spain's Hydrographic Institute. In the intertidal areas the charts were complemented with local 1:5000 cartography – more precisely, with maps 00718d, 00188d and 00281d from the Galician regional government. On the vertical axis the σ-coordinate approach was adopted, with 12 σ-layers.

Details of the calibration and validation of the model may be found in [69, 82]. The TSE index [59] shows a hotspot for tidal stream energy in the narrow passage between Pt. Postiña and Pt. Cabalar (Figure 2.14).

The flow velocity in the area around the hotspot is shown in Figure 2.15 at two levels in the water column, the surface and bottom σ-layers, and at two moments of the tidal cycle, mid-flood and mid-ebb. Peak velocities are well above $1.5\,\text{m}\,\text{s}^{-1}$, with greater values in the surface layer than in the bottom layer – as expected. Importantly, mid-flood velocities are substantially larger than mid-ebb velocities. This tidal asymmetry, which is present not only in many rias in NW Spain [79] but, more generally, in many estuaries worldwide, is of great relevance in terms of tidal stream power. As indicated, the fact that tidal stream power varies with the cube of the current speed, equation (2.31), implies that a relatively modest difference in terms of current speed translates into a substantial difference in terms of power.

In determining the nominal (installed) power of the tidal stream turbines to be deployed at a tidal farm, the developers should not aim to fully exploit the power peaks in the flow, for this would lead to rated power being attained only a small percentage of

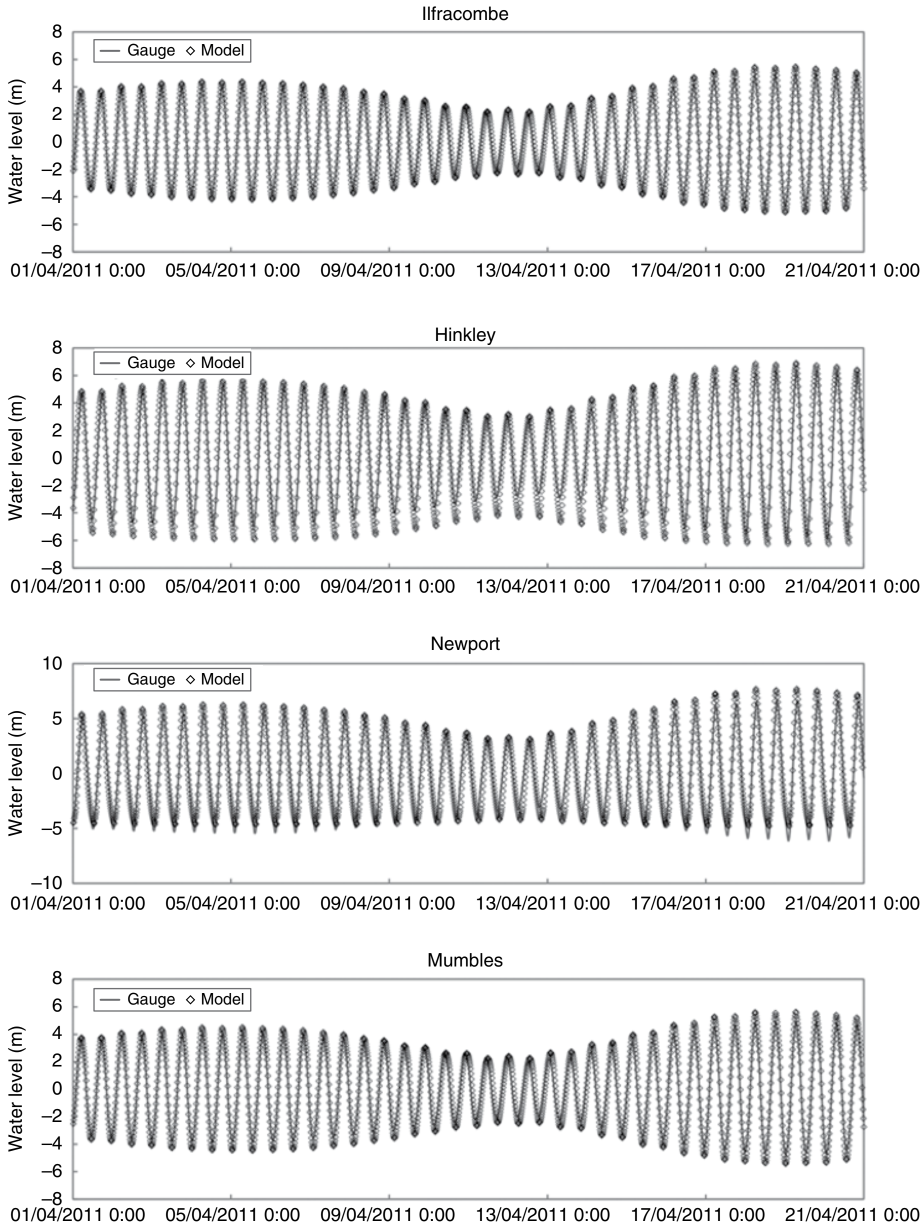

Figure 2.10 Model validation: observed (gauge) and computed (model) time series of tidal levels at four stations in the Bristol Channel.

the time, and consequently to low capacity factors and higher costs [68]. Indeed, the selection of the turbines and generators must take into account not only technical but also economic and functional constraints [17, 62]. The variability of the flow may be considered in selecting the turbines by means of a parametric approach [70].

Table 2.2 Correlation coefficient (*R*) and RMSE values of predicted and measured currents.

Location		*R*	RMSE[a]
Site F	Spring tide	0.9054	0.1406
(51° 33.3′ N,	Neap tide	0.8908	0.1568
3° 56.9′ W)	Direction	0.9956	4.5546
Site G	Spring tide	0.8770	0.2241
(51° 27′ N,	Neap tide	0.8853	0.1543
3° 55.6′ W)	Direction	0.9948	9.9818
Site H	Spring tide	0.8960	0.1646
(51° 32.5′ N,	Neap tide	0.9170	0.1239
3° 53.5′ W)	Direction	0.8966	13.4300
Site K	Spring tide	0.8581	0.2833
(51° 20.1′ N,	Neap tide	0.9062	0.1475
3° 50.3′ W)	Direction	0.8911	15.231
Site L	Spring tide	0.8689	0.3436
(51° 16′ N,	Neap tide	0.8702	0.2163
3° 47.4′ W)	Direction	0.9946	9.4107

a) RMSE values in metres per second for the spring and neap tidal velocities, and in degrees for the direction.

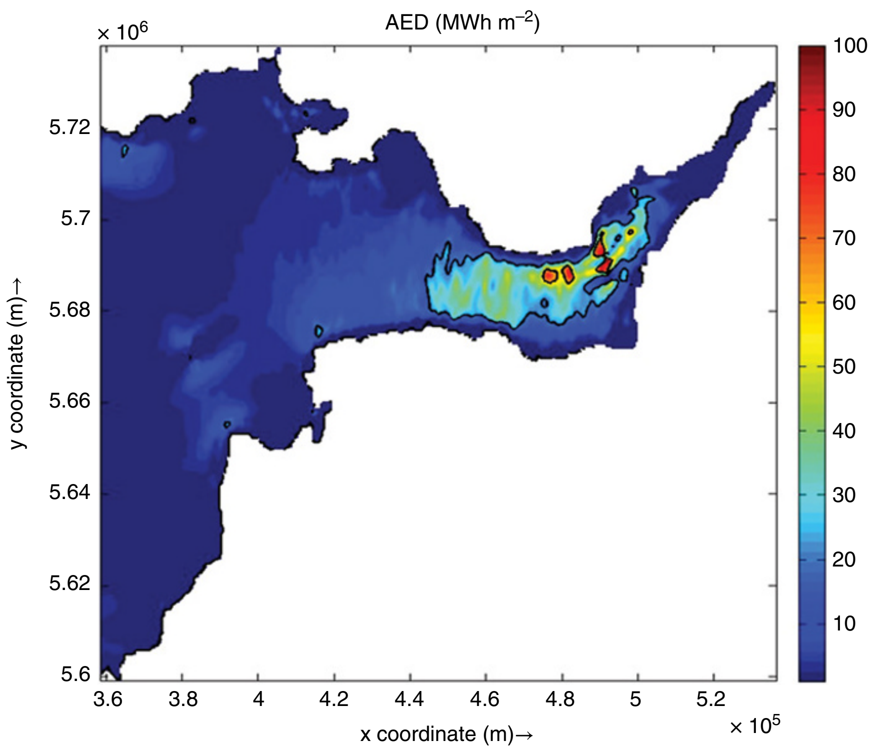

Figure 2.11 Annual tidal stream energy density (MWh m^{-2}) in the Severn Estuary and Bristol Channel (UK).

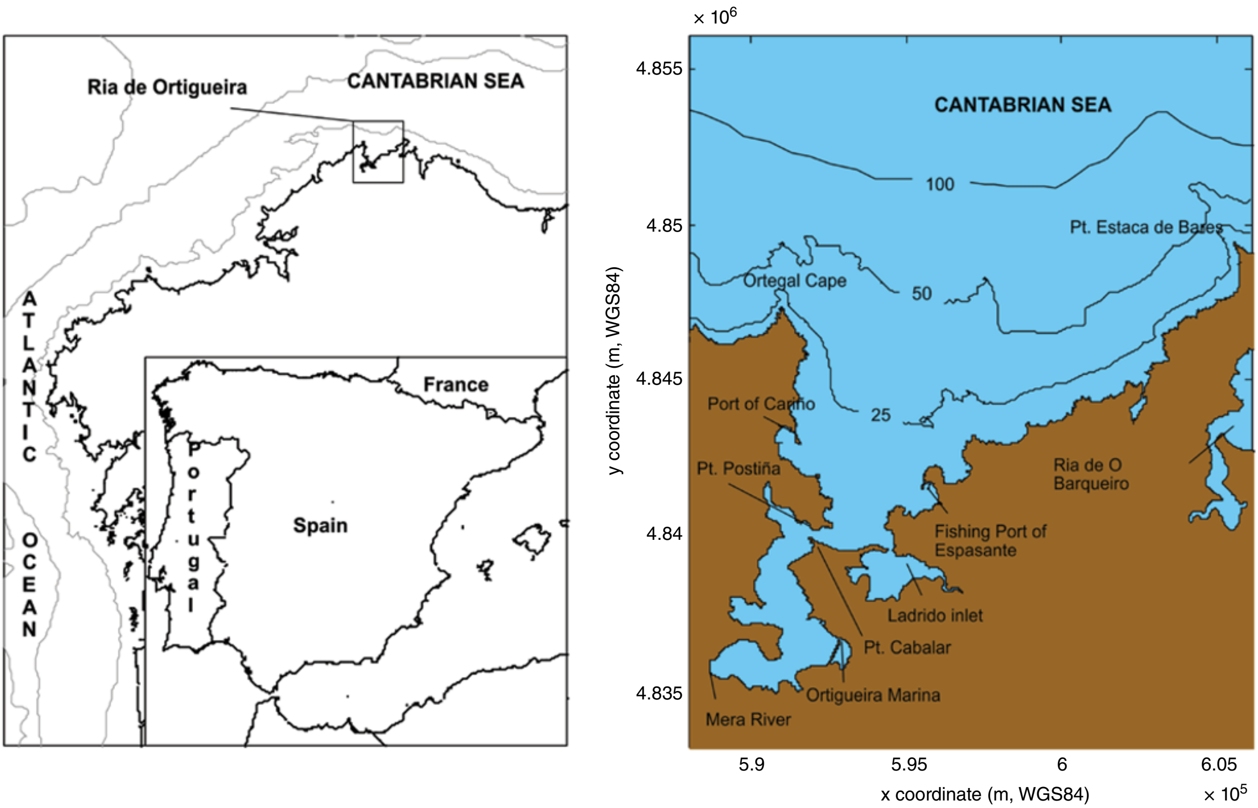

Figure 2.12 Ria de Ortigueira, Galicia (NW Spain).

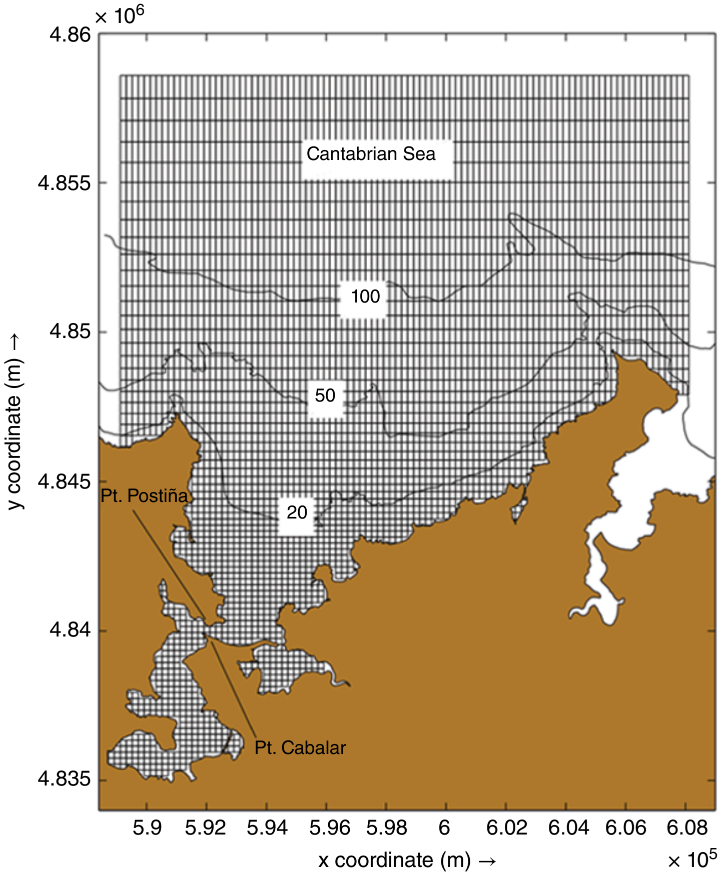

Figure 2.13 Computational grid of Ria de Ortigueira (NW Spain).

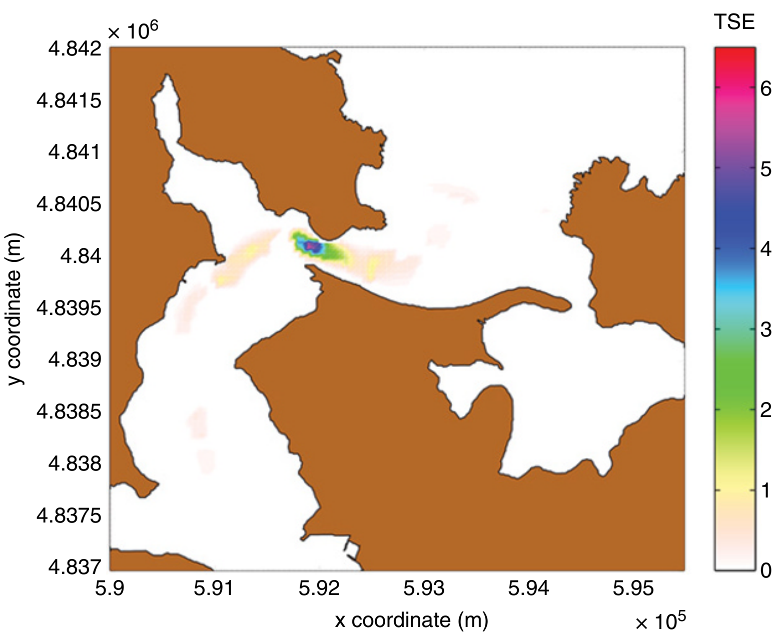

Figure 2.14 TSE index in the inner estuary. The area with greatest potential for tidal stream exploitation between Pt. Postiña and Pt. Cabalar (Figure 2.13) is conspicuous in the graph.

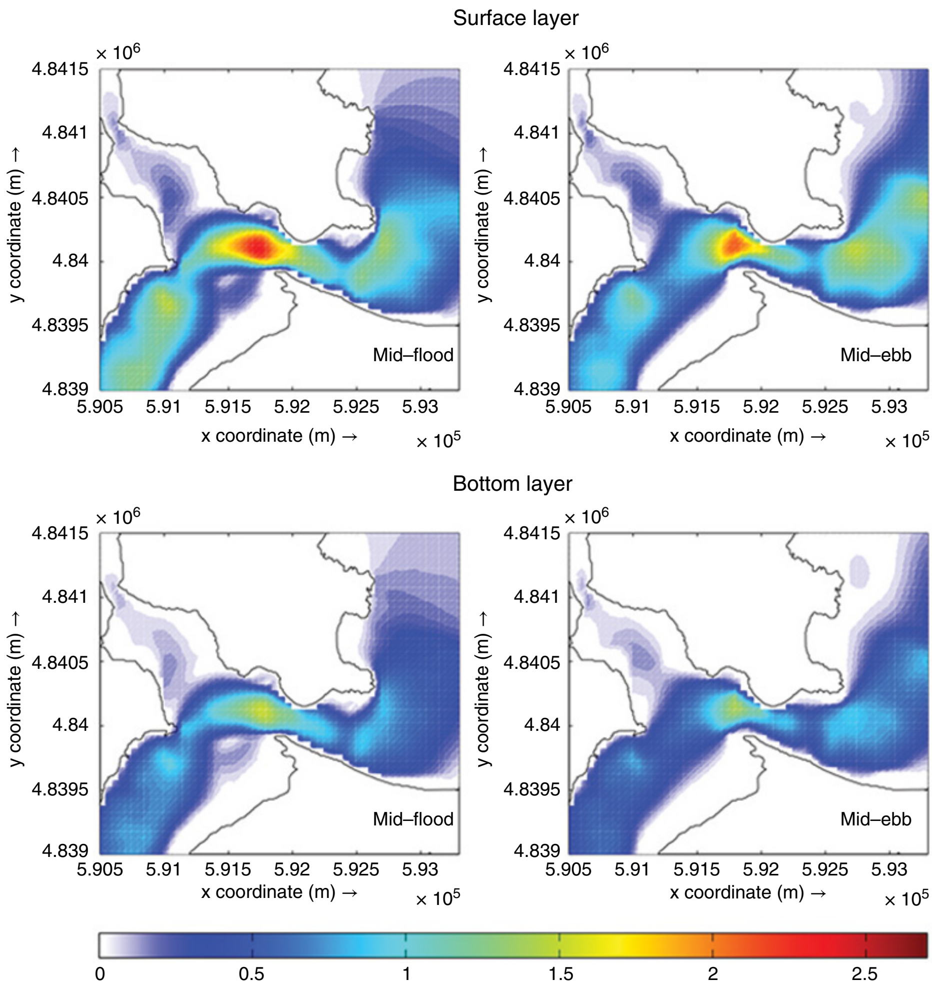

Figure 2.15 Flow velocity at mid-flood and mid-ebb in the surface and bottom layers of the inner estuary, Ria de Ortigueira (NW Spain).

Acknowledgements

The author is indebted to N. Arean, M. Sanchez and Dr R. Carballo for their help with the figures and computation, and to Spain's State Ports and the British Oceanographic Data Centre for kindly providing data.

References

1 Iglesias G, López M, Carballo R, Castro A, Fraguela JA, Frigaard P. Wave energy potential in Galicia (NW Spain). *Renewable Energy* 2009;34:2323–33.
2 Carballo R, Sánchez M, Ramos V, Fraguela J, Iglesias G. The intra-annual variability in the performance of wave energy converters: A comparative study in N Galicia (Spain). *Energy* 2015;82:138–46.

3 Kinsman B. *Wind Waves: Their Generation and Propagation on the Ocean Surface.* Dover; 2002.

4 Mørk G, Barstow S, Kabuth A, Pontes MT. Assessing the global wave energy potential. *ASME 2010 29th International Conference on Ocean, Offshore and Arctic Engineering* (pp. 447–54). American Society of Mechanical Engineers; 2010.

5 Fernandez H, Iglesias G, Carballo R, Castro A, Fraguela J, Taveira-Pinto F, *et al.* The new wave energy converter WaveCat: Concept and laboratory tests. *Marine Structures* 2012;29:58–70.

6 Iglesias G, Fernández H, Carballo R, Castro A, Taveira-Pinto F. The WaveCat© – Development of a new wave energy converter. *World Renewable Energy Congress 2011: Marine and Ocean Technology* 2011;9:2151–8.

7 Vicinanza D, Margheritini L, Kofoed JP, Buccino M. The SSG wave energy converter: Performance, status and recent developments. *Energies* 2012;5:193–226.

8 Margheritini L, Vicinanza D, Frigaard P. SSG wave energy converter: Design, reliability and hydraulic performance of an innovative overtopping device. *Renewable Energy* 2009;34:1371-80.

9 Rusu E, Guedes Soares C. Numerical modelling to estimate the spatial distribution of the wave energy in the Portuguese nearshore. *Renewable Energy* 2009;34:1501–16.

10 Vicinanza D, Cappietti L, Ferrante V, Contestabile P. Estimation of the wave energy in the Italian offshore. *Journal of Coastal Research* 2011; SI 61:613–617.

11 Vicinanza D, Contestabile P, Ferrante V. Wave energy potential in the north-west of Sardinia (Italy). *Renewable Energy* 2013;50:506–21.

12 Pontes MT. Assessing the European wave energy resource. *Journal of Offshore Mechanics and Arctic Engineering* 1998;120:226–31.

13 Iglesias G, Carballo R. Wave energy potential along the Death Coast (Spain). *Energy* 2009;34:1963–75.

14 Astariz S, Iglesias G. The economics of wave energy: A review. *Renewable and Sustainable Energy Reviews* 2015;45:397–408.

15 Astariz S, Iglesias G. Wave energy vs. other energy sources: A reassessment of the economics. *International Journal of Green Energy* 2016;13:747–55.

16 Astariz S, Vazquez A, Iglesias G. Evaluation and comparison of the levelized cost of tidal, wave, and offshore wind energy. *Journal of Renewable and Sustainable Energy* 2015;7:053112.

17 Vazquez A, Iglesias G. LCOE (levelised cost of energy) mapping: A new geospatial tool for tidal stream energy. *Energy* 2015;91:192–201.

18 Astariz S, Iglesias G. Enhancing wave energy competitiveness through co-located wind and wave energy farms. A review on the shadow effect. *Energies* 2015;8:7344–66.

19 Astariz S, Iglesias G. Accessibility for operation and maintenance tasks in co-located wind and wave energy farms with non-uniformly distributed arrays. *Energy Conversion and Management* 2015;106:1219–29.

20 Astariz S, Iglesias G. Output power smoothing and reduced downtime period by combined wind and wave energy farms. *Energy* 2016;97:69–81.

21 Astariz S, Perez-Collazo C, Abanades J, Iglesias G. Hybrid wave and offshore wind farms: A comparative case study of co-located layouts. *International Journal of Marine Energy* 2016;15:2–16.

22 Astariz S, Perez-Collazo C, Abanades J, Iglesias G. Co-located wind-wave farm synergies (operation & maintenance): A case study. *Energy Conversion and Management* 2015;91:63–75.